

UC Davis

UC Davis Previously Published Works

Title

Elite Control, Gut CD4 T Cell Sparing, and Enhanced Mucosal T Cell Responses in *Macaca nemestrina* Infected by a Simian Immunodeficiency Virus Lacking a gp41 Trafficking Motif

Permalink

<https://escholarship.org/uc/item/19x6b92m>

Journal

Journal of Virology, 89(20)

ISSN

0022-538X

Authors

Breed, Matthew W
Elser, Samra E
Torben, Workineh
et al.

Publication Date


2015-10-15

DOI

10.1128/jvi.01134-15

Peer reviewed

Elite Control, Gut CD4 T Cell Sparing, and Enhanced Mucosal T Cell Responses in *Macaca nemestrina* Infected by a Simian Immunodeficiency Virus Lacking a gp41 Trafficking Motif

Matthew W. Breed,^{a*} Samra E. Elser,^b Workineh Torben,^a Andrea P. O. Jordan,^b Pyone P. Aye,^a Cecily Midkiff,^a Faith Schiro,^a Chie Sugimoto,^a Xavier Alvarez-Hernandez,^a Robert V. Blair,^a Anoma Somasunderam,^c Netanya S. Utay,^c Marcelo J. Kuroda,^a Bapi Pahar,^a Roger W. Wiseman,^d David H. O'Connor,^d Celia C. LaBranche,^e David C. Montefiori,^e Mark Marsh,^f Yuan Li,^g Michael Piatak, Jr.,^g Jeffrey D. Lifson,^g Brandon F. Keele,^g Patricia N. Fultz,^h Andrew A. Lackner,^a  James A. Hoxie^b

Tulane National Primate Research Center, Covington, Louisiana, USA^a; Perelman School of Medicine, University of Pennsylvania, Philadelphia, Pennsylvania, USA^b; Baylor College of Medicine, Houston, Texas, USA^c; University of Wisconsin National Primate Research Center, Madison, Wisconsin, USA^d; Duke University Medical Center, Durham, North Carolina, USA^e; MRC Laboratory for Molecular Cell Biology, University College, London, United Kingdom^f; AIDS and Cancer Virus Program, Leidos Biomedical Research, Inc., Frederick National Laboratory for Cancer Research, Frederick, Maryland, USA^g; University of Alabama at Birmingham, Birmingham, Alabama, USA^h

ABSTRACT

Deletion of Gly-720 and Tyr-721 from a highly conserved GYxxØ trafficking signal in the SIVmac239 envelope glycoprotein cytoplasmic domain, producing a virus termed ΔGY, leads to a striking perturbation in pathogenesis in rhesus macaques (*Macaca mulatta*). Infected macaques develop immune activation and progress to AIDS, but with only limited and transient infection of intestinal CD4⁺ T cells and an absence of microbial translocation. Here we evaluated ΔGY in pig-tailed macaques (*Macaca nemestrina*), a species in which SIVmac239 infection typically leads to increased immune activation and more rapid progression to AIDS than in rhesus macaques. In pig-tailed macaques, ΔGY also replicated acutely to high peak plasma RNA levels identical to those for SIVmac239 and caused only transient infection of CD4⁺ T cells in the gut lamina propria and no microbial translocation. However, in marked contrast to rhesus macaques, 19 of 21 pig-tailed macaques controlled ΔGY replication with plasma viral loads of <15 to 50 RNA copies/ml. CD4⁺ T cells were preserved in blood and gut for up to 100 weeks with no immune activation or disease progression. Robust antiviral CD4⁺ T cell responses were seen, particularly in the gut. Anti-CD8 antibody depletion demonstrated CD8⁺ cellular control of viral replication. Two pig-tailed macaques progressed to disease with persisting viremia and possible compensatory mutations in the cytoplasmic tail. These studies demonstrate a marked perturbation in pathogenesis caused by ΔGY's ablation of the GYxxØ trafficking motif and reveal, paradoxically, that viral control is enhanced in a macaque species typically predisposed to more pathogenic manifestations of simian immunodeficiency virus (SIV) infection.

IMPORTANCE

The pathogenesis of human immunodeficiency virus (HIV) and simian immunodeficiency virus (SIV) reflects a balance between viral replication, host innate and adaptive antiviral immune responses, and sustained immune activation that in humans and Asian macaques is associated with persistent viremia, immune escape, and AIDS. Among nonhuman primates, pig-tailed macaques following SIV infection are predisposed to more rapid disease progression than are rhesus macaques. Here, we show that disruption of a conserved tyrosine-based cellular trafficking motif in the viral transmembrane envelope glycoprotein cytoplasmic tail leads in pig-tailed macaques to a unique phenotype in which high levels of acute viral replication are followed by elite control, robust cellular responses in mucosal tissues, and no disease. Paradoxically, control of this virus in rhesus macaques is only partial, and progression to AIDS occurs. This novel model should provide a powerful tool to help identify host-specific determinants for viral control with potential relevance for vaccine development.

Hallmarks of human immunodeficiency virus type 1 (HIV-1) infection and pathogenic models of simian immunodeficiency virus (SIV) infection in Asian macaques include early targeting and rapid depletion of CD4⁺ effector memory T cells that express the chemokine receptor CCR5, particularly in gut lymphoid tissue where they are abundant (1). A subsequent loss of epithelial barrier function and translocation of microbial products to the systemic circulation contributes to generalized immune activation, which likely generates new CD4⁺ target T cells that serve to sustain ongoing viral replication (2). With associated contributions from macrophage and dendritic cell dysfunction (3–6), a state of persistent immune activation and inflammation is established. These processes, coupled with viral escape from adap-

tive immune responses, lead to persistent and progressive infection and depletion of central memory CD4⁺ T cells and an eventual loss of CD4⁺ T cell regenerative capacity (2) that underlies progression to AIDS.

Among nonhuman primate models, marked differences in the outcome of SIV infection have been observed, reflecting a complex interplay of viral and host factors (1, 7, 8). SIV infection of several African monkey species that are natural hosts of different SIV strains results in only a transient depletion of mucosal CD4⁺ T cells, with limited immune activation and little or no disease despite ongoing viral replication (9–11). However, even among Asian macaque species that succumb to pathogenic SIV infection, differences in the natural history of infection have been observed.

In Chinese rhesus macaques, SIVmac infection leads to disease in approximately two-thirds of animals, with the other one-third controlling plasma viral RNA to low or undetectable levels (12–14), while in Indian rhesus macaques, viral replication levels are on average significantly higher and progression to disease is more commonly seen and occurs more rapidly, although the rate of progression can be modulated in the setting of protective major histocompatibility complex (MHC) class I alleles (15, 16). Pig-tailed macaques (*Macaca nemestrina*) have been shown to be particularly sensitive to pathogenic effects of SIVmac and SIVagm infection and typically exhibit a more uniform and rapid progression to disease and death than do rhesus macaques (8, 17–19). The enhanced pathogenicity of SIV infection seen in this species has been attributed to an increased basal level of immune activation caused by a “leaky” gut epithelial barrier and elevated baseline microbial translocation in animals prior to infection (20, 21). This increased basal immune activation likely enhances viral replication and accelerates disease progression (17, 20). Transcriptional profiling of lymphoid tissues during acute SIVagm infection of pig-tailed macaques, which leads rapidly to AIDS, has revealed a markedly robust and sustained expression of mRNAs associated with cellular stress pathways, type I and II interferon (IFN) responses, and T and B cell activation (18). Pig-tailed macaques also exhibit a mutated Trim5- α gene due to retrotransposition of the cyclophilin A gene between exons 7 and 8, which ablates the restriction of some SIVs and HIV-1s seen in other macaque species (22, 23) and could contribute to a more uniform progression to AIDS in this species.

Our laboratories have described *in vivo* effects on the pathogenic molecular clone SIVmac239 of a mutation in a highly conserved tyrosine-dependent GYxx \emptyset trafficking motif within the envelope glycoprotein (Env) cytoplasmic domain (where x is any amino acid and \emptyset is an amino acid with a bulky hydrophobic side chain) (24, 25). This virus, termed Δ GY, contains a deletion of Gly-720 and Tyr-721 from this motif (GYRPV) and in rhesus macaques exhibits a striking phenotype in which it acutely replicates, comparably to SIVmac239, with high levels of virus in plasma and organized lymphoid tissue (e.g., lymph nodes, spleen, tonsils, and Peyer’s patches), but fails to infect macrophages and, remarkably, exhibits only limited and transient infection of gut

CD4⁺ T cells in lamina propria (24), which are rapidly depleted during wild-type SIVmac239 infection (26, 27). With a sparing of gut-associated lymphoid tissue and a lack of CD4⁺ T cell depletion in this compartment, gut epithelial barrier function is maintained, and there is no microbial translocation. However, although rhesus macaques infected with Δ GY exhibit viral RNA levels 2 to 3 logs lower than those with SIVmac239 during chronic infection, ongoing viral replication is associated with systemic immune activation that occurs even in the absence of gut damage, and animals progress to AIDS in association with novel and possibly compensatory mutations in the envelope cytoplasmic domain (24, 28). These findings indicate that while epithelial damage and systemic translocation of microbial products have been associated with chronic immune activation and disease progression, these processes are not absolutely required for immunopathogenesis and additional factors can contribute. The work also demonstrated a remarkable alteration of cellular and tissue tropism of infection caused by the Δ GY mutation within the GYxx \emptyset trafficking motif, leading to sparing of mucosal CD4⁺ T cells and no detectable macrophage infection (24).

In the current study, we evaluated the effects of Δ GY infection in pig-tailed macaques, in which SIV infection is typically more pathogenic than in rhesus macaques. We found that infection in pig-tailed macaques was similar to infection in rhesus macaques: this virus established a high acute peak of viremia, largely spared CD4⁺ T cells in intestinal lamina propria, and failed to cause detectable infection of tissue macrophages. However, Δ GY viremia in pig-tailed macaques contrasted markedly with that in rhesus macaques. In pig-tailed macaques, Δ GY viremia was rapidly suppressed in the majority of animals to levels of <15 to 50 copies/ml, with preservation of CD4⁺ T cells in blood and gut for >100 weeks. Anti-CD8 cell depletion studies suggested that host control of Δ GY was, at least in part, mediated by CD8⁺ cells. However, this control was also strongly associated with the appearance of robust, SIV-specific CD4⁺ T cell responses, particularly in intestinal lamina propria, which was spared during acute Δ GY infection. These findings extend the novel *in vivo* effects of the Δ GY mutation in the SIV Env cytoplasmic domain and reveal a paradoxical species-specific difference in rhesus compared to pig-tailed macaques, with superior control occurring in pig-tailed macaques, a species that typically exhibits more rapid disease progression following wild-type SIV infection.

Received 5 May 2015 Accepted 14 July 2015

Accepted manuscript posted online 29 July 2015

Citation Breed MW, Elser SE, Torben W, Jordan APO, Aye PP, Midkiff C, Schiro F, Sugimoto C, Alvarez-Hernandez X, Blair RV, Somasunderam A, Utay NS, Kuroda MJ, Pahar B, Wiseman RW, O’Connor DH, LaBranche CC, Montefiori DC, Marsh M, Li Y, Piatak M, Jr, Lifson JD, Keele BF, Fultz PN, Lackner AA, Hoxie JA. 2015. Elite control, gut CD4 T cell sparing, and enhanced mucosal T cell responses in *Macaca nemestrina* infected by a simian immunodeficiency virus lacking a gp41 trafficking motif. *J Virol* 89:10156–10175. doi:10.1128/JVI.01134-15.

Editor: F. Kirchhoff

Address correspondence to James A. Hoxie, hoxie@mail.med.upenn.edu.

* Present address: Matthew W. Breed, Laboratory Animal Sciences Program, Leidos Biomedical Research, Inc., Frederick National Laboratory for Cancer Research, Bethesda, Maryland, USA.

Supplemental material for this article may be found at <http://dx.doi.org/10.1128/JVI.01134-15>.

Copyright © 2015, American Society for Microbiology. All Rights Reserved.

doi:10.1128/JVI.01134-15

MATERIALS AND METHODS

Ethics statement. The Tulane and University of Alabama at Birmingham (UAB) Institutional Animal Care and Use Committees approved all experiments using rhesus and pig-tailed macaques (protocols P0088R and P0147 at Tulane and 041205386 at UAB). The Tulane National Primate Research Center (TNPRC) and UAB facilities are accredited by the Association for Assessment and Accreditation of Laboratory Animal Care International and closely follow the recommendations made in the *Guide for the Care and Use of Laboratory Animals* (29). The NIH Office of Laboratory Animal Welfare assurance number for TNPRC is A4499-01, and that for UAB is A3255-01. All clinical procedures, including administration of anesthesia and analgesics, were carried out under the direction of a laboratory animal veterinarian. Animals were anesthetized with 10 mg/kg ketamine hydrochloride for blood collection procedures. Laboratory animal veterinarians performed intestinal resections and lymph node biopsies. Animals were preanesthetized with acepromazine and glycopyrolate, anesthesia was induced with either 10 mg/kg ketamine hydrochloride or 8 mg/kg tiletamine-zolazepam, and animals were then intubated and main-

TABLE 1 Summary of animals, virus stock, outcome, and experimental group for ΔGY- and control SIVmac239-infected pig-tailed macaques

Group	Animal ^a	Sex ^b	Status	Euthanasia (wk)	Haplotypes ^c	
					Mane-A	Mane-B
ΔGY	GC07	M	Controller		A061, A084	B016b, B044
	GC72	M	Controller		A063, A084	B016b, B104
	GG10	M	Controller		A074, A084	B118a, B118a
	GR26	M	Progressor	74	A016, A052	B028, B123
	GR29	M	Controller		A063, A084	B016b, B044
	HA94	M	Progressor	76	A006, A082	B016a, B118b
	HC67	M	Controller		A052, A084	B028, B069
	HJ98	M	Controller		A082, A082	B016a, B028
	JV12	M	Controller		A019, A052	B043, B120
	JV13	M	Controller	38	A039, A084	B004, B080
	JV14	M	Controller		A022, A082	B017a, B111
	JV15	M	Controller	16	Not determined	Not determined
	JV16	M	Controller		A006, A082	B016b, B028
	JV17	M	Controller		A052, A087	B015, B028
	JV18	M	Controller		A009, A084	B*024, B041
	JV19	M	Controller		A032, A071	B017c, B120
	AT36	M	Controller		A019, A084	B017b, B015
	AT4D	M	Controller		A006, A009	B043, B104
	CT2B	M	Controller		A082, A084	B056, B104
	CT2L	M	Controller		A004, A006	B017b, B052
CT2J	M	Controller		A006, A082	B016a, B052	
SIVmac239	GR06	M	AIDS	51	A052, A061	B028, B104
	GR08	F	AIDS	51	A007, A084	B118a, B118b
	IK37	M	AIDS	25	A019, A061	B016b, B052
	IP82	F	AIDS	27	A010, A084	B027, B044
	AD7C	M	AIDS	76	A082, A082	B043, B118b
	AK93	M	AIDS	77	A082, A084	B007, B015
	99P040	M	AIDS	112	Not determined	Not determined
	99P041	M	AIDS	93	Not determined	Not determined
	99P051	M	AIDS	89	Not determined	Not determined

^a Bold text indicates pig-tailed macaques that progressed to disease.

^b M, male; F, female.

^c The A084 and B017 MHC haplotypes have been associated with exceptional control of chronic-phase SIV replication in a subset of macaques (41–43).

tained on a mixture of isoflurane and oxygen. Buprenorphine was given intraoperatively and postoperatively for analgesia. All possible measures are taken to minimize discomfort of all the animals used in this study. Animals were closely monitored daily following surgery for any signs of illness, and appropriate medical care was provided as needed. Euthanasia was performed in accordance with the recommendations of the panel on Euthanasia of the American Veterinary Medical Association. Tulane University and UAB comply with NIH policy on animal welfare, the Animal Welfare Act, and all other applicable federal, state, and local laws.

Animals, viral inoculations, and sample collection. A total of 30 pig-tailed macaques were used in this study and were inoculated intravenously (i.v.) with 100 50% tissue culture infective dose (TCID₅₀) of ΔGY ($n = 21$) or 100 TCID₅₀ of SIVmac239 ($n = 9$) (Table 1). Before any procedure, macaques were anesthetized by an intramuscular injection of ketamine hydrochloride (10 mg/kg). For inoculations performed at the Tulane National Primate Research Center (TNPRC), viruses were produced in 293T cells transfected with plasmids containing full-length proviral DNA. For inoculations performed at the University of Alabama at Birmingham (UAB), viruses were grown in CEMx174 cells. ΔGY-infected animals AT36, AT4D, CT2B, CT2L, and CT2J were maintained at UAB, whereas all other ΔGY-infected animals were maintained at TNPRC (Table 1). Viruses were quantified by determining TCID₅₀ on rhesus macaque peripheral blood mononuclear cells (PBMCs). Ten macaques were housed at UAB (5 infected with ΔGY and 5 with SIVmac239), and 20 were housed at TNPRC (16 infected with ΔGY and 4 with SIVmac239). A group of 17

Indian-origin rhesus macaques housed at TNPRC and described in a previous study (24) were used as a control group and were inoculated with ΔGY (8 animals with 100 TCID₅₀ i.v. and 1 animal with 350 TCID₅₀ intravaginally) or SIVmac239 (8 animals with 100 TCID₅₀ i.v.). Prior to use, all animals tested negative for antibodies to SIV, simian T cell leukemia virus (STLV), and type D retrovirus and by PCR for type D retrovirus. Multiple blood samples and small intestinal biopsy samples (endoscopic duodenal pinch biopsy samples or jejunal resection biopsy samples) were collected under anesthesia (ketamine hydrochloride or isoflurane) at various times from each animal (see the figures and figure legends). Animals were euthanized if they exhibited a loss of more than 25% of maximum body weight, anorexia for more than 4 days, or major organ failure or medical conditions unresponsive to treatment (e.g., severe pneumonia or diarrhea).

All animals were maintained at TNPRC or UAB in accordance with standards of the Association for Assessment and Accreditation of Laboratory Animal Care and the *Guide for the Care and Use of Laboratory Animals* prepared by the National Research Council (29). The UAB and TNPRC Institutional Animal Care and Use Committees approved all studies.

Quantitation of viral load in plasma. Plasma viral loads were determined at various times using a reverse transcription-PCR (RT-PCR) assay with a limit of detection of between 15 and 70 SIV RNA copies/ml (30). Plasma viral load determination in rhesus macaques was performed by a branched DNA (bDNA) assay (Siemens Diagnostics, Emeryville, CA) with a limit of detection of 125 or 700 SIV RNA copies/ml (24).

Lymphocyte isolation from intestinal tissues. Intestinal cells were collected either by endoscopic pinch biopsies of the small intestine or by 2-cm surgical resections of the jejunum from animals at various times. Intestinal biopsy procedures and isolation of cells from intestinal tissues were described previously (12, 31–33). Intestinal cells were isolated using EDTA-collagenase digestion and Percoll density gradient centrifugation.

Immunophenotyping and analysis of cell turnover with BrdU. Immunophenotyping of cells was performed on isolated lamina propria lymphocytes (LPLs) and anticoagulated whole blood using antibodies reactive with CD3 (SP34), CD8 (SK1 or SK2), CD4 (L200), CD14 (M5E2), CD45 (MB4-6D6), CD20 (B9E9), 5-bromo-2'-deoxyuridine (BrdU) (3D4), and HLA-DR (L234), all from BD Biosciences, San Jose, CA. Additional antibodies included anti-CD8 (3B5) (Invitrogen, Carlsbad, CA), -CD20 (Beckman Coulter, Indianapolis, IN), and -CD45 (Miltenyi Biotech, San Diego, CA). Viability was determined using LIVE/DEAD stain (L34957) (Life Technologies, Grand Island, NY). Protocols for performing immunophenotyping have been described previously (24). CD4⁺ and CD8⁺ lymphocytes and monocytes were further analyzed for turnover and immune activation. For turnover experiments, BrdU (Sigma) was administered to animals, as described previously (34, 35). Pig-tailed macaques, infected with Δ GY ($n = 8$) or SIVmac239 ($n = 4$), had BrdU administered before infection and at multiple times postinfection; at least a month for washout was allotted between BrdU inoculations. Control groups for the BrdU labeling experiments included naive, Δ GY-infected, or SIVmac-infected rhesus macaques (24, 34). Flow cytometry data were analyzed using FlowJo software version 9.1 (TreeStar Inc., Ashland, OR).

Intracellular cytokine analysis. Intracellular cytokine analysis of SIV-specific CD4 and CD8 peripheral blood and lamina propria lymphocytes was performed in a subset of the 19 Δ GY-controlling pig-tailed macaques, at week 66 for animals GC07, GC72, GG10, GR29, HC67, and HJ98 and before and 8 weeks after CD8⁺ depletion for HC67 and HJ98, as described previously (36, 37). An additional four pig-tailed macaques infected with SIVmac239 (GR06, GR08, IK37, and IP82) were similarly assessed for SIV-specific CD4 and CD8 responses in peripheral blood. Briefly, cells were stimulated with SIV peptides (Env, Gag, or Pol; NIH AIDS Research & Reference Reagent Program), and then brefeldin A (Sigma) was added. Medium was used as a negative control, and phorbol myristate acetate (PMA)-Ionomycin was used as a positive control. Cells were stained with anti-CD3 (SP34), -CD4 (L200), and -CD8 (5H10) and a viability stain (L34957) and then washed, permeabilized, and stained with antibodies to interleukin-2 (IL-2) (MQ1-17H12), IFN- γ (4S.B3), and tumor necrosis factor alpha (TNF- α) (MA611) (BD Biosciences, San Jose, CA). Cells were fixed in stabilizing fixative buffer (BD Biosciences, San Jose, CA) and analyzed on a Becton Dickinson LSR II flow cytometer.

The gating strategy was similar to the immunophenotyping described above. In brief, cells were gated first on singlets, lymphocytes, followed by live cells, and then on CD3⁺ T cells and subsequently on CD3⁺ CD4⁺ and CD3⁺ CD8⁺ T cell subsets. The percentages of IFN- γ -, TNF- α -, and IL-2-positive responses in each subset against each antigen as well as negative or positive controls were assessed using FlowJo software, version 9.1 (TreeStar). The analysis of absolute cytokine expression was performed with PESTLE and SPICE software version 5.3 (J. Nozzi and M. Roederer, VRC, NIAID, Bioinformatics and Computational Biosciences Branch). Final presentations of total cytokine responses were prepared in GraphPad Prism v5.0c (GraphPad Software, Inc., La Jolla, CA).

CD8⁺ cell depletion. CD8⁺ cell depletion protocols were performed on Δ GY-controlling pig-tailed macaques at TNPRC (on animals HC67 and HJ98, at week 81) and at UAB (on animals AT36 and AT4D, at week 97). Animals received anti-CD8 antibodies MT807R1 (at TNPRC) or cM-T807 (at UAB), provided by the Nonhuman Primate Reagent Resource (Boston, MA). Antibodies were administered subcutaneously (s.c.) at 10 mg/kg on day 0 and i.v. at 5 mg/kg on days 3, 7, and 10. CD8⁺ T cells in blood were monitored by flow cytometry, as described above.

Analysis of plasma LPS and sCD14 levels. To measure lipopolysaccharide (LPS), plasma samples (collected in EDTA) were diluted to 10%

in endotoxin-free water, heated to 80°C for 10 min, and then quantified in duplicate with a commercially available *Limulus* amoebocyte lysate assay (Lonza, Basel, Switzerland) (38, 39). Plasma soluble CD14 (sCD14) was determined using a commercially available enzyme-linked immunosorbent assay (ELISA) (R&D Systems, Minneapolis, MN). Samples were diluted to 0.5% and tested in duplicate, as described previously (40).

MHC typing of pig-tailed macaques. MHC class I genotyping was carried out as described previously (41–43). Total cellular RNA was isolated from whole blood or PBMCs, and first-strand cDNA was synthesized by reverse transcription with SuperScript III (Life Technologies, USA). This cDNA served as a template for PCR with SBT568 primers that bind conserved sequences flanking the highly polymorphic peptide-binding domain and universally amplify macaque MHC class I transcripts. After pyrosequencing of these amplicons on a GS Junior instrument (Roche/454, USA), a custom genotyping workflow was used to map the resulting sequences against a curated database of known *Macaca nemestrina* (Mane) class I sequences. Ancestral Mane-A and Mane-B haplotypes were inferred on the basis of the combinations of class I alleles that were identified for each animal as described previously (Table 1) (41–43).

Assays for neutralizing antibodies. Neutralizing antibody responses were determined on viruses produced in 293T cells using TZM-bl cells expressing CD4 and CCR5. All assays were conducted in triplicate as described previously (44). The 50% inhibitory dilution (ID₅₀) was calculated as the reciprocal serum dilution causing 50% reduction of relative light units compared with the virus alone (without test sample). Viruses used in the neutralization panel included SIVmac239 and SIVmac251.6 (45) and variants of SIVsmE660 that are neutralization sensitive (SIVsmE660-VTRN) or neutralization resistant (SIVsmE660-2A5) (46). Neutralization-sensitive SIVsmE660-2A5.VTRN was generated by introducing 4 amino acid changes into neutralization-resistant SIVsmE660-2A5 that have been shown previously to confer this phenotype (46).

ISH. Tissue samples collected at biopsy or necropsy were fixed in Z-Fix (Anatech, Battle Creek, MI) and embedded in paraffin, and 5- μ m-thick sections were cut from select tissues and adhered to charged glass slides. SIV RNA *in situ* hybridization (ISH) was then performed, as described previously (24, 28, 47, 48), using SIV RNA sense/antisense probes tagged with digoxigenin (DIG) and obtained from Lofstrand Laboratories (Gaithersburg, MD) or provided by Jake Estes (AIDS and Cancer Virus Program at the Frederick National Laboratory of Cancer Research) (49). The chromogens used were nitroblue tetrazolium (NBT)–5-bromo-4-chloro-3-indolylphosphate (BCIP) for light microscopy or liquid permanent red for fluorescence microscopy. Results were assessed by bright-field optical microscopy (DM LB microscope [Leica, Buffalo Grove, IL] and spot imaging [camera and software from Insight, Sterling Heights, MO]) or confocal microscopy (Leica TCS SP2 confocal microscope equipped with three lasers [Leica Microsystems, Buffalo Grove, IL]).

Confocal microscopy. Double- and triple-label confocal microscopy was performed to colocalize SIV RNA with cell type-specific markers to determine the immunophenotype of infected cells, as described previously (47). Immunofluorescent labeling of T cells (rabbit polyclonal to CD3 [Biocare Medical, Concord, CA]), CD4⁺ memory T cells (mouse IgG1 monoclonal to OPD4/CD45RO [Dako]), macrophages (mouse IgG1 monoclonal to CD68 [Dako] or CD163 [Serotec]), and BrdU (rat monoclonal BU/1/75 [Novus Biologicals]) was performed after ISH, as previously described (24, 28, 34, 47, 50, 51). After incubation with the primary antibodies (anti-CD3, anti-OPD4/CD45RO [which only detects CD45RO on CD4⁺ T cells {34}], anti-CD68, anti-CD163, or anti-BrdU) and subsequent washes, the appropriate species-specific secondary antibodies were applied (Alexa Fluor 488- or 633-conjugated goat anti-rabbit or goat anti-mouse IgG1 or goat anti-rat [Invitrogen, Carlsbad, CA]). Confocal microscopy was performed using the sequential mode to capture separately the fluorescence from the different fluorochromes (Leica Microsystems, Exton, PA). NIH Image v1.62 and Adobe Photoshop v7 software were used to correct the colors collected in the different channels: Alexa 488 (green), Alexa 568 (red), Alexa 633 (blue), and differential

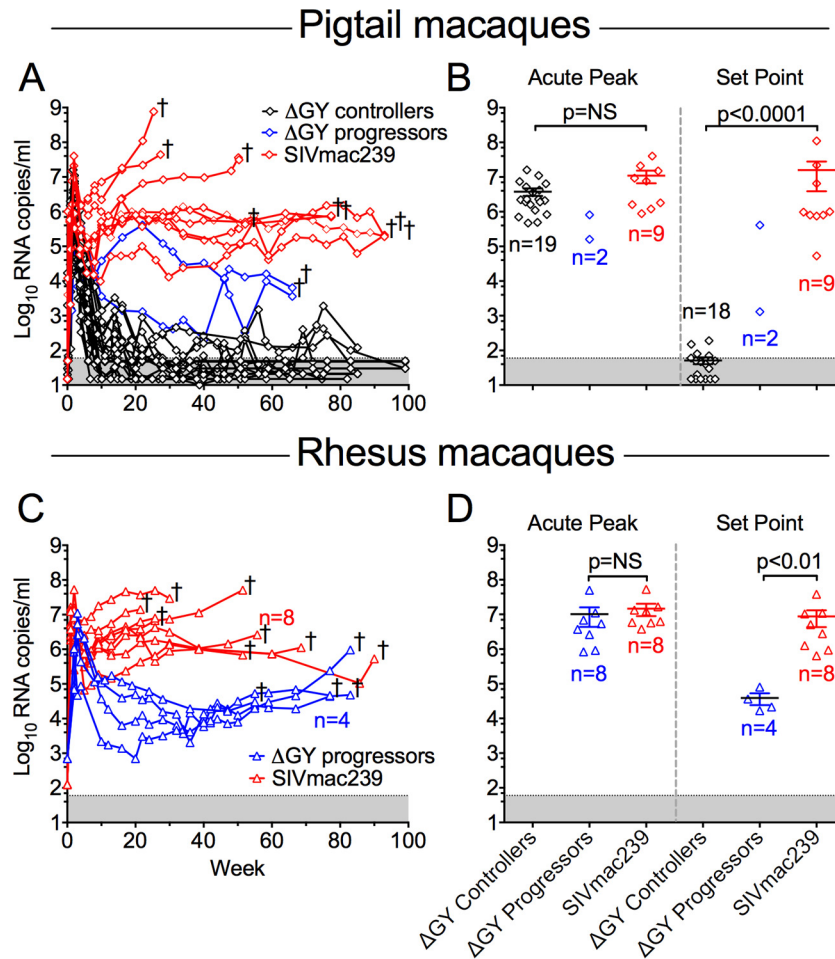


FIG 1 Plasma viral loads in pig-tailed and rhesus macaques infected with Δ GY or SIVmac239. Plasma viral loads are shown for pigtailed macaques (A and B) (diamonds) and previously reported rhesus macaques (C and D) (triangles), (24). †, time points at which individual animals were euthanized with AIDS. (A and C) Plasma RNA levels postinfection. One Δ GY-infected pig-tailed macaque (JV15) died of causes unrelated to SIV infection at week 16 with a plasma viral RNA level of 200 copies/ml and is not included in the viral set point analysis (see Fig. S1A in the supplemental material). (B and D) Peak viremia and viral set points for individual animals (mean \pm SEM). Δ GY-infected macaques were divided into controllers (black) or progressors (blue); SIVmac239-infected animals are shown (red). The threshold of sensitivity for the viral RNA assay varied from 15 to 50 RNA copies/ml and is represented by the shaded area. RNA values for individual animals are shown in Fig. S1 in the supplemental material. P[r] values were determined using the Mann-Whitney nonparametric test. NS, not significant.

interference contrast (DIC) (gray scale). In selected animals and tissues, the numbers of infected cells by phenotype were quantitated as described previously (24).

SGA analysis. Single genome amplification (SGA) analyses were performed on plasma samples from two Δ GY-infected pig-tailed macaques that progressed to disease (GR26 and HA94): GR26 at weeks 2, 6, 22, and 58 after infection and from HA94 at week 76 at necropsy. For two animals that were controlling infection (HC67 and HJ98), SGA analyses were performed at the plasma viral RNA peak at 2 weeks after CD8⁺ cell depletion. The entire *env* gene was sequenced using a limiting-dilution PCR to ensure that only one amplifiable molecule was present in each reaction mixture, as previously described (24, 52). Sequence alignments were generated with Clustal W and presented as highlighter plots (www.hiv.lanl.gov). Unrooted neighbor-joining trees were constructed in Clustal W, excluding gaps and correcting for multiple substitutions. APOBEC signature mutations were identified with HyperMut (www.hiv.lanl.gov), and diversity/divergence measurements were determined using pairwise comparisons implemented in DIVEIN (53).

Statistical analysis. All statistical analyses were performed using GraphPad Prism v5.0c (GraphPad Software, Inc., La Jolla, CA). The non-

parametric Mann-Whitney test was used to determine *P* values when comparing two groups that were not normally distributed.

Nucleotide sequence accession numbers. All sequences in this study were deposited in GenBank (accession numbers KP313060 to KP313239).

RESULTS

Viral dynamics of Δ GY infection in pig-tailed macaques. Pig-tailed macaques were inoculated intravenously (i.v.) with SIVmac239 or Δ GY, and analyses were performed on blood, small intestinal biopsy specimens (excisional or endoscopic), and tissues collected at necropsy. Plasma viral loads for Δ GY- or SIVmac239-infected animals are shown in Fig. 1A. As expected, all SIVmac239-infected animals developed high acute viral peaks (mean \pm standard error of the mean [SEM], $1.1 \times 10^7 \pm 4.3 \times 10^6$ RNA copies/ml) followed by high viral set points ($1.6 \times 10^7 \pm 1.2 \times 10^7$ RNA copies/ml), defined as the geometric mean of plasma viral RNA at 20 weeks after infection (Fig. 1B; see Fig. S1C in the supplemental material). Δ GY-infected pig-tailed macaques developed a comparably high acute RNA peak ($3.8 \times 10^6 \pm 9.2 \times$

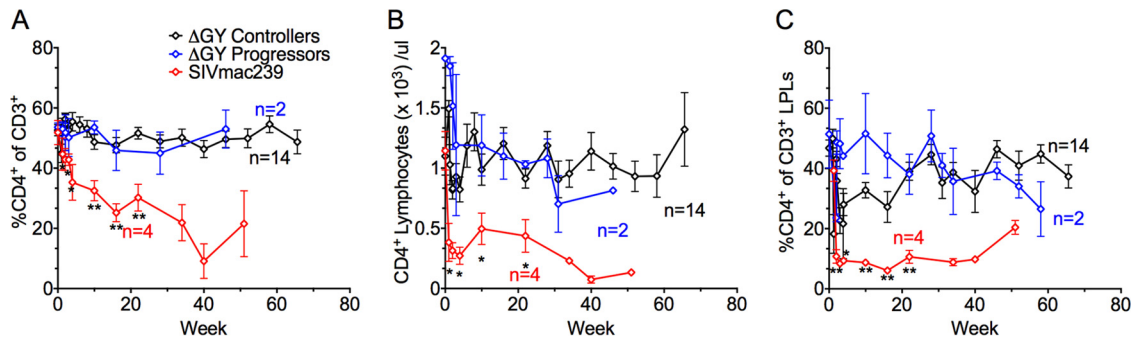


FIG 2 Changes in mean percent and absolute number of peripheral blood CD4⁺ T lymphocytes and mean percent gut mucosal CD4⁺ T lymphocytes in pig-tailed macaques over time. The mean percent (A) and absolute (B) CD4⁺ T lymphocyte levels from whole blood and the mean percent CD4⁺ T lymphocytes from the gut lamina propria (C) are shown for pig-tail macaque ΔGY-infected controllers (black), ΔGY-infected progressors (blue), and SIVmac239-infected naive controls (red). (A) The percentage of CD4⁺ T lymphocytes in whole blood progressively declined in the SIVmac239 control group but remained stable for both ΔGY-controlling and -progressing animals. (B) The absolute number of CD4⁺ T lymphocytes in whole blood remained stable for the ΔGY-infected controllers, decreased in the ΔGY-infected progressors late in the course of infection, and fell rapidly in the SIVmac239-infected group. (C) The percentage of gut lamina propria CD4⁺ T lymphocytes decreased rapidly for the SIVmac239 group. For the ΔGY-infected progressors and controllers there was a mild reduction during acute infection with subsequent recovery to preinfection levels. While the ΔGY-infected controllers maintained gut lamina propria CD4⁺ T lymphocytes through chronic infection, a late decline was observed in the ΔGY-infected progressors at week 60. *, $P < 0.05$; **, $P < 0.01$ (between ΔGY-infected controller and SIVmac239 groups). P values were determined using the Mann-Whitney nonparametric test.

10⁵) (Fig. 1; see Fig. S1A in the supplemental material). However, in striking contrast to SIVmac239 infection, the set-point viral load was significantly lower in ΔGY-infected animals ($P < 0.0001$), with 90% (19 of 21) of animals controlling viremia to ≤ 100 RNA copies/ml. Of these 19 controlling animals, 15 exhibited levels below detection (≤ 15 or 50 copies/ml using a standard assay or a more sensitive assay), with the other 4 animals showing persisting but low level viremia with intermittent RNA increases of 10^2 to 10^3 copies/ml.

Deep-sequencing analysis showed that animals in both the ΔGY and SIVmac239 challenge groups carried a diverse array of MHC haplotypes (Table 1), indicating that differences in control of chronic-phase viral replication were unlikely to be associated with MHC class I genetics, including the Mane-A084 allele (formerly Mane-A*10), which has been implicated as an SIVmac-controlling allele in pig-tailed macaques in early (54) although not more recent (41, 55) studies. Viral set points for ΔGY-controlling pig-tailed macaques were also reduced compared to those in 4 previously described ΔGY-infected rhesus macaques ($P < 0.01$), which had RNA levels of $3.8 \times 10^4 \pm 1.4 \times 10^4$ copies/ml and progressed to disease (Fig. 1C and D) (24).

Two of 21 ΔGY-infected pig-tailed macaques (GR26 and HA94) (Table 1) exhibited higher set-point viremia (4.1×10^5 and 1.3×10^3 RNA copies/ml, respectively) and progressed to simian AIDS-associated disease by approximately 70 weeks postinfection (Fig. 1A; see Fig. S1B in the supplemental material). At necropsy, both had evidence of SIV infection, including generalized lymphoid hyperplasia and thrombocytopenia, pulmonary arteriopathy, and thrombosis (56–58), despite only slight reductions in numbers and percentages of CD4⁺ T cells in blood and gut lamina propria (see below). In contrast, SIVmac239-infected animals exhibited findings typical of simian AIDS, with one or more of the following: meningoencephalitis with multinucleated giant cells, severe anemia and thrombocytopenia, giant cell pneumonia, esophageal candidiasis, and intranuclear inclusion bodies consistent with cytomegalovirus infection.

Two ΔGY-infected pig-tailed macaques that controlled infection (JV13 and JV15) were euthanized due to complications unrelated to SIV infection. JV13 had recurrent rectal prolapse and

was euthanized at week 38 with a viral load of < 15 copies/ml; JV15 had a testicular torsion at week 15 and was euthanized with a viral load of 200 copies/ml that was rapidly declining (see Fig. S1 in the supplemental material).

Thus, in marked contrast to ΔGY infection in rhesus macaques and SIVmac239 infection in rhesus and pig-tailed macaques, ΔGY infection was highly controlled in $> 90\%$ of pig-tailed macaques, despite exhibiting acute viral RNA peaks that were identical to those of SIVmac239. This finding was both unexpected and remarkable given the typically more rapid progression to disease in SIVmac-infected pig-tailed than in rhesus macaques (17–19).

Peripheral and gut CD4⁺ T cells in ΔGY-infected pig-tailed macaques are maintained throughout infection. A characteristic of pathogenic SIV and HIV infection is a gradual and progressive decline in peripheral blood CD4⁺ T cells during chronic infection and a rapid loss of gut CD4⁺ T cells in intestinal lamina propria during acute infection (27, 59–62). In blood, SIVmac239-infected pig-tailed macaques exhibited a decrease in the number and percentage of CD4⁺ T cells, while ΔGY-controlling animals showed stable levels of CD4⁺ T cells throughout infection (Fig. 2A and B). Remarkably, in lamina propria, while SIVmac239-infected animals showed the typical rapid loss of CD4⁺ T cells (Fig. 2C), ΔGY-infected animals displayed only a modest decrease (Fig. 2C), which recovered to preinfection levels by week 30 and remained relatively stable for up to 70 weeks postinfection (Fig. 2C). This mild and transient acute reduction in CD4⁺ T cells was similar to that previously seen in ΔGY-infected rhesus macaques (24). Interestingly, even in the two ΔGY-infected animals that progressed to disease, there was only a modest reduction in lamina propria CD4⁺ T cells (17.4% for HA94 and 35.6% for GR26) (Fig. 2C), and peripheral CD4⁺ T cells remained stable (Fig. 2A and B). Thus, in pig-tailed macaques, although ΔGY infection produced a high acute peak of plasma viremia comparable to that of SIVmac239s, it caused only a mild and transient acute loss of gut CD4⁺ T cells, and CD4⁺ T cells in blood and gut remained stable during chronic infection.

Characterization of ΔGY-infected cells in gastrointestinal lymphoid tissue during acute infection. Small intestinal biopsy specimens were obtained during acute infection (up to day 28

postinfection), and *in situ* hybridization (ISH) for SIV RNA and immunohistochemistry were performed to evaluate the distribution and immunophenotype of Δ GY-infected cells. At day 7, infected cells were not identified despite detectable, albeit moderate, levels of RNA in plasma (Fig. 3A) (110 , 1.6×10^3 , and 3×10^4 copies/ml for animals GR29, GC07, and GG10, respectively [Fig. 1A; see Fig. S1 in the supplemental material]). By day 15, infected cells were present but were sparsely distributed in a patchy, multifocal pattern throughout immune inductive sites (organized lymphoid nodules and Peyer's patches) and effector sites (lamina propria and epithelium) (Fig. 3B). By day 21 (not shown) and day 28 (Fig. 3C), infected cells were detectable only at low levels in immune inductive sites (Peyer's patches) but were absent throughout the diffuse lamina propria. This finding was remarkable but agrees with the observation that $CD4^+$ T cells in gut lamina propria were only mildly depleted from preinfection levels (Fig. 2C). These results were in contrast to those for small intestinal biopsy specimens from SIVmac239-infected pig-tailed macaques, where extensive and diffuse infection throughout the lamina propria occurs during acute infection (references 17 and 20 and data not shown), corresponding to the massive and rapid depletion of $CD4^+$ T cells from this site (Fig. 2C).

To identify the immunophenotype of Δ GY-infected cells in gastrointestinal tissues, we performed multilabel confocal microscopy on jejunum at day 15 using antibodies to CD3 (T cells), CD68 and CD163 (macrophages), CD45RO (memory $CD4^+$ T cells) (50), and BrdU (proliferating cells) and digoxigenin-labeled probes to detect SIV RNA (Fig. 3D and E). As expected, T cells, including memory ($CD45RO^+$) and proliferating ($BrdU^+$) cells (Fig. 3E), were infected. In addition, although macrophages that had phagocytosed SIV-infected T cells were observed (Fig. 3D), SIV-infected macrophages were rare in Δ GY- compared to SIVmac239-infected animals. At day 163, for SIVmac239, 14.9% of $CD68^+$ cells were positive for SIV RNA, whereas for Δ GY, only 0.42% were positive (Fig. 3F and data not shown).

Thus, while Δ GY infection of intestinal lamina propria $CD4^+$ T cells occurred during acute infection, similar to Δ GY infection in rhesus macaques and in marked contrast to SIVmac239 infection in both macaque species, infection was transient and sparsely distributed in this compartment, with no detectable infection beyond day 28 and no macrophage infection (24, 28).

Progressive infection for Δ GY is altered compared to that for SIVmac239. As noted above, although the majority of Δ GY-infected pig-tailed macaques controlled Δ GY infection and retained normal numbers of gut and peripheral $CD4^+$ T cells, two animals (GR26 and HA94) progressed to disease. Tissues at necropsy were analyzed by ISH for SIV RNA and compared to necropsy samples from 4 SIVmac239-infected pig-tailed macaques that progressed to AIDS (Fig. 4). All SIVmac239-infected animals exhibited high levels of plasma RNA at necropsy ($2.1 \times 10^8 \pm 1.8 \times 10^8$ copies/ml [mean \pm SEM]), and viral RNA in tissues was abundant throughout the small and large intestines, lymph nodes, spleen, and brain (selected images are shown in Fig. 4). In contrast, both Δ GY-infected animals that progressed to disease (referred to as Δ GY-progressing animals below) exhibited more moderate levels of plasma RNA at necropsy (3.6×10^3 and 6.4×10^3 copies/ml for GR26 and HA94, respectively) (see Fig. S1B in the supplemental material), and viral infection was difficult to detect, with only rare

infected cells detected in mesenteric lymph nodes and none detected in intestine or brain (Fig. 4).

Evaluation of immune activation and microbial translocation in Δ GY-controlling pig-tailed macaques. Increased monocyte turnover (34, 35), chronic immune activation (5, 38, 63), and microbial translocation (5, 38) are correlates of disease progression in virulent HIV and SIV infection. Given the transient nature of Δ GY's infection in lamina propria and early sparing of $CD4^+$ T cells from this site, parameters of cellular turnover, immune activation, and microbial translocation were evaluated in Δ GY-controlling, Δ GY-progressing, and SIVmac239-infected pig-tailed macaques.

BrdU incorporation in peripheral blood $CD4^+$ and $CD8^+$ T cells and in $CD14^+$ monocytes was assessed as an indicator of cell turnover (34, 51). SIVmac239-infected pig-tailed macaques exhibited an early and sustained elevation in $BrdU^+$ cells, particularly $CD8^+$ T cells and monocytes, with a more variable incorporation in $CD4^+$ T cells. In contrast, Δ GY-controlling macaques exhibited little to no increase in BrdU incorporation in any of these cell types (Fig. 5A to C). Both Δ GY-progressing macaques displayed late increases in $CD8^+$ and $CD4^+$ T cell turnover, although the small numbers precluded statistical comparisons (Fig. 5A and B). With the exception of a single point at week 34 for animal GR26, no increase in monocyte turnover was seen for Δ GY-progressing pig-tailed macaques (Fig. 5C).

HLA-DR expression on $CD8^+$ and $CD4^+$ T cells was also followed as a marker of T cell activation (Fig. 5D and E) and was increased on $CD8^+$ T cells of all SIVmac239-infected pig-tailed macaques, while minimal changes occurred in Δ GY-controlling animals. Consistent with increased $CD8^+$ T cell turnover in both Δ GY-progressing animals, a trend toward increased HLA-DR expression was observed at late time points prior to necropsy (Fig. 5D). A similar, although less striking, increase was observed for $CD4^+$ T cells (Fig. 5E).

BrdU incorporation in T cells and monocytes in Δ GY- and SIVmac239-infected pig-tailed macaques was compared to results previously reported for these viruses in rhesus macaques (24) (Fig. 5F, G, and H). Although viral set points for Δ GY were reduced in rhesus macaques compared to those for SIVmac239, replication continued, and all chronically infected animals ultimately progressed ($n = 4$) (24). Despite the small number of animals, $CD8^+$ and $CD4^+$ T cell turnover was increased in Δ GY-infected rhesus macaques compared to Δ GY-infected pig-tailed macaques (Fig. 5F and G). However, in both macaque species there was little if any evidence of elevated monocyte turnover during Δ GY infection, in contrast to that in SIVmac239 infection (Fig. 5H).

Microbial translocation was evaluated in Δ GY-controlling ($n = 14$) and SIVmac239-infected ($n = 4$) animals by measuring the levels of soluble CD14 (sCD14) and lipopolysaccharide (LPS) in plasma. As is typical of pathogenic SIV infection (38), sCD14 progressively increased during SIVmac239 infection (Fig. 6A and B), while no change from preinfection levels occurred for Δ GY-infected animals (Fig. 6). Although not statistically significant, similar trends were found for plasma LPS, where a modest increase from preinfection levels was seen in SIVmac239-infected animals while Δ GY-infected animals appeared to remain unchanged (Fig. 6C and D).

Δ GY controllers exhibit robust SIV-specific $CD4^+$ and $CD8^+$ T cell responses in peripheral blood and intestinal mucosa. To assess correlates of Δ GY control, we examined SIV-specific $CD4^+$ and $CD8^+$ T cell cytokine responses at week 66 after

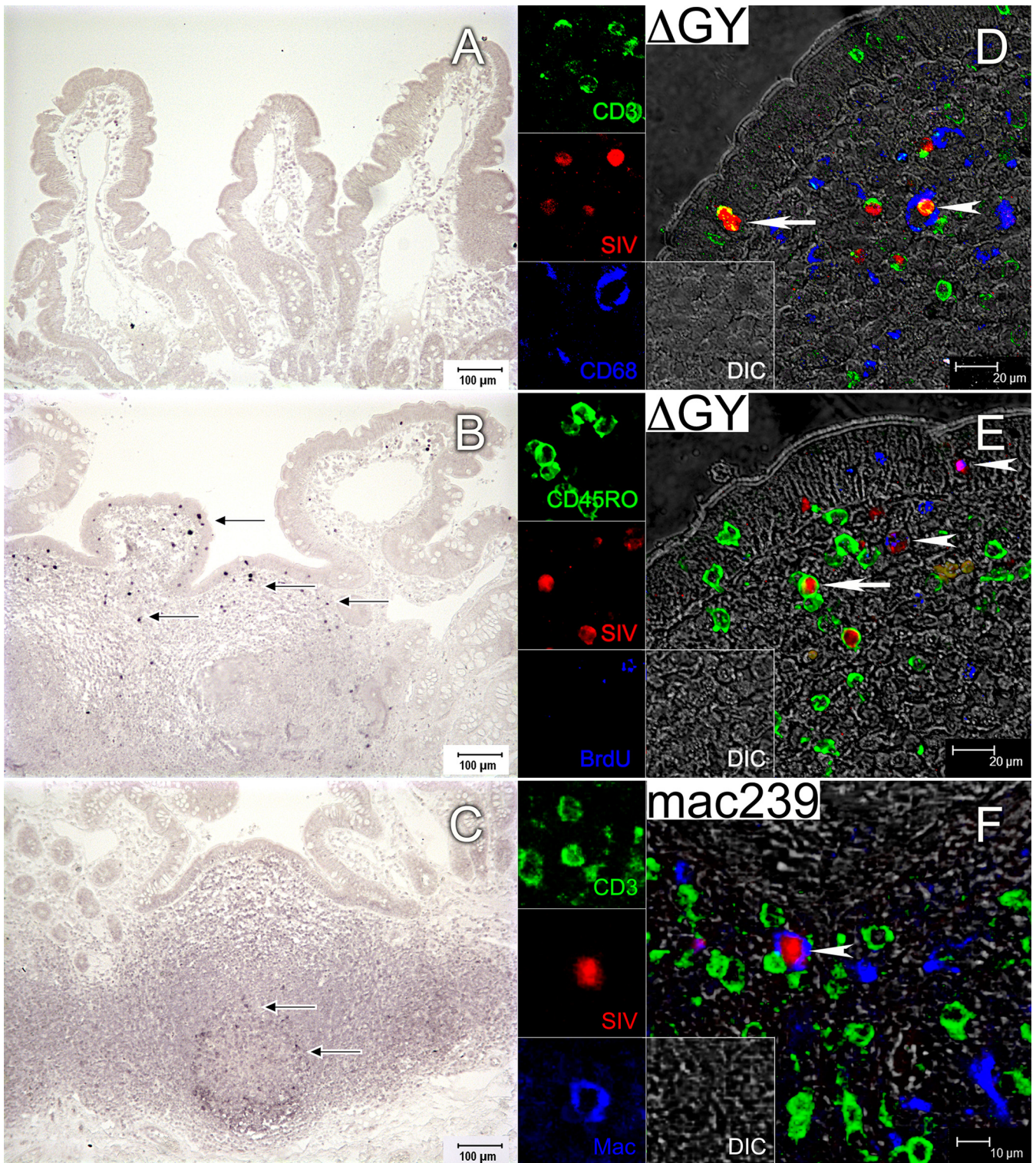


FIG 3 Localization and immunophenotype of Δ GY-infected cells in the small intestine during acute infection in pig-tailed macaques. (A to C) Localization of SIV RNA in jejunum from Δ GY-infected pig-tailed macaques by *in situ* hybridization (ISH). Representative ISH images from biopsy specimens collected from three animals at day 7, two animals at day 15, and two animals at day 28 are shown. Black arrows indicate infected cells. Infected cells were undetectable at day 28 (C). (D to F) Immunophenotyping by multilabel confocal microscopy of SIV-infected cells in jejunum from a Δ GY-infected animal at day 15 (D and E) and from an SIVmac239-infected animal at day 28 (F). For each panel, the individual channels are shown on the left and the larger merged image is shown on the right. (D) All Δ GY-infected cells were CD3⁺, indicated by a yellow color in the merged image (white arrow and arrowhead). No SIV-infected macrophages were present (blue); however, a white arrowhead shows a CD68⁺ macrophage phagocytosing an infected CD3⁺ cell. (E) Memory T cells (CD45RO⁺) (white arrow) and proliferating cells (BrdU⁺) (white arrowheads) are infected with Δ GY. (F) SIVmac239-infected macrophages (CD68 and CD163) are clearly detectable (white arrowhead).

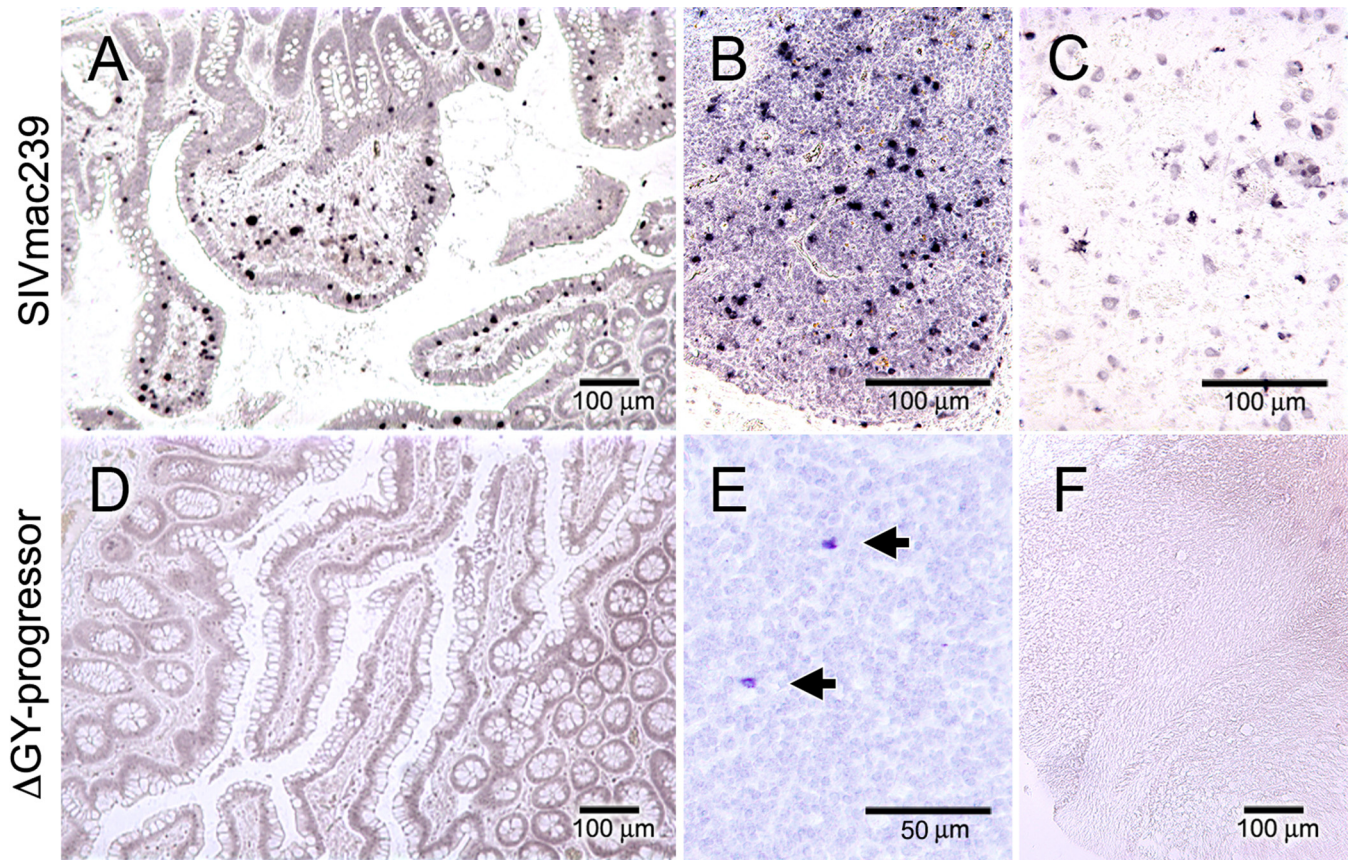


FIG 4 Localization of SIVmac239- and Δ GY-infected cells at necropsy in pig-tailed macaques with disease progression. SIV RNA *in situ* hybridization was performed at necropsy on jejunum (A and D), mesenteric lymph nodes (B and E), and brain tissue (C and F) from pig-tailed macaques IK37 infected with SIVmac239 with AIDS (top row) and GR26 infected with Δ GY (bottom row) with disease progression. Representative ISH images from necropsy samples collected from the four animals infected with SIVmac239 (IK37, IP82, GR06, and GR08) and the two animals that progressed to disease with Δ GY (GR26 and HA94) are shown. In SIVmac239 infection, numerous infected cells are diffusely scattered throughout the jejunum, lymph node, and brain (week 25). In the Δ GY-progressing animals, infected cells were not detectable in jejunum or brain and were only rarely present in mesenteric lymph nodes (arrows; week 74).

Δ GY infection in blood and gut from 6 pig-tailed macaques that had been controlling Δ GY to levels of <15 to 30 copies/ml for approximately 1 year. Results for intracellular cytokine expression of IFN- γ , IL-2, and TNF- α for peripheral blood or gut CD4⁺ and CD8⁺ T cells following stimulation with pools of SIV Gag, Pol, or Env peptides (36, 37) are shown (Fig. 7).

Although there was variability among specific cytokine responses and in the viral components targeted, in peripheral blood, CD4⁺ T cells were reactive, with responses ranging from 0 to 2.3% to Gag, Pol, and/or Env (Fig. 7). However, in all animals there were remarkably strong and broad responses in gut CD4⁺ T cells, especially toward Gag and Pol (Fig. 7). GC72 exhibited the strongest responses, with up to 19% of cells producing IL-2 to Gag peptides and approximately 7% producing IFN- γ to Pol peptides. GG10 also had strong gut CD4⁺ T cell responses, with approximately 1 to 2% of cells producing IFN- γ to Env and Pol peptides. CD8⁺ T cell responses in blood and gut were generally lower than CD4⁺ T cell responses, although animal GC72 displayed strong responses to Gag peptides in peripheral blood (2.7%, IFN- γ) and gut (15%, IL-2) and strong responses to Pol peptides in gut (1.5 to 6%, IFN- γ and TNF- α) (Fig. 7). Thus, despite having undetectable viral loads for >70 weeks, Δ GY-infected controlling animals exhibited robust SIV-specific T cell responses that were greater for

CD4⁺ than for CD8⁺ T cells and greater in cells from gut mucosal tissue than in those from peripheral blood. In contrast, animals infected with SIVmac239 had consistently lower CD4 and CD8 T cell responses (<0.4%) to Gag, Pol, and Env in peripheral blood (not shown) despite higher viral loads (see Fig. S1C in the supplemental material). The rapid and profound depletion of mucosal CD4⁺ T cells (Fig. 2) precluded an assessment of mucosal responses in these animals.

Role of CD8 cellular responses in Δ GY control. In 4 pig-tailed macaques that had maintained undetectable levels of plasma virus (<15 to 50 RNA copies/ml), CD8⁺ cells were depleted using an anti-CD8 monoclonal antibody. Two animals (AT36 and AT4D) were depleted at week 97 following infection, and two animals (HC67 and HJ98) were depleted at week 82. Plasma viral RNA increased in all 4 animals to peaks of 2.5×10^4 , 5.4×10^3 , 1.2×10^5 , and 1.7×10^5 copies/ml within 2 weeks of antibody treatment, corresponding to the decline in CD8⁺ T cells. With recovery of these cells, viral control was reestablished in all 4 animals (Fig. 8A, B, and C). In two animals, HC67 and HJ98, CD8⁺ T cell cytokine responses to Gag, Pol, and Env peptides after CD8⁺ T cell recovery increased markedly compared to predepletion levels (Fig. 8D versus E), consistent with a strong anamnestic response. Thus, although Δ GY was controlled for 1.6 to 1.8 years to levels

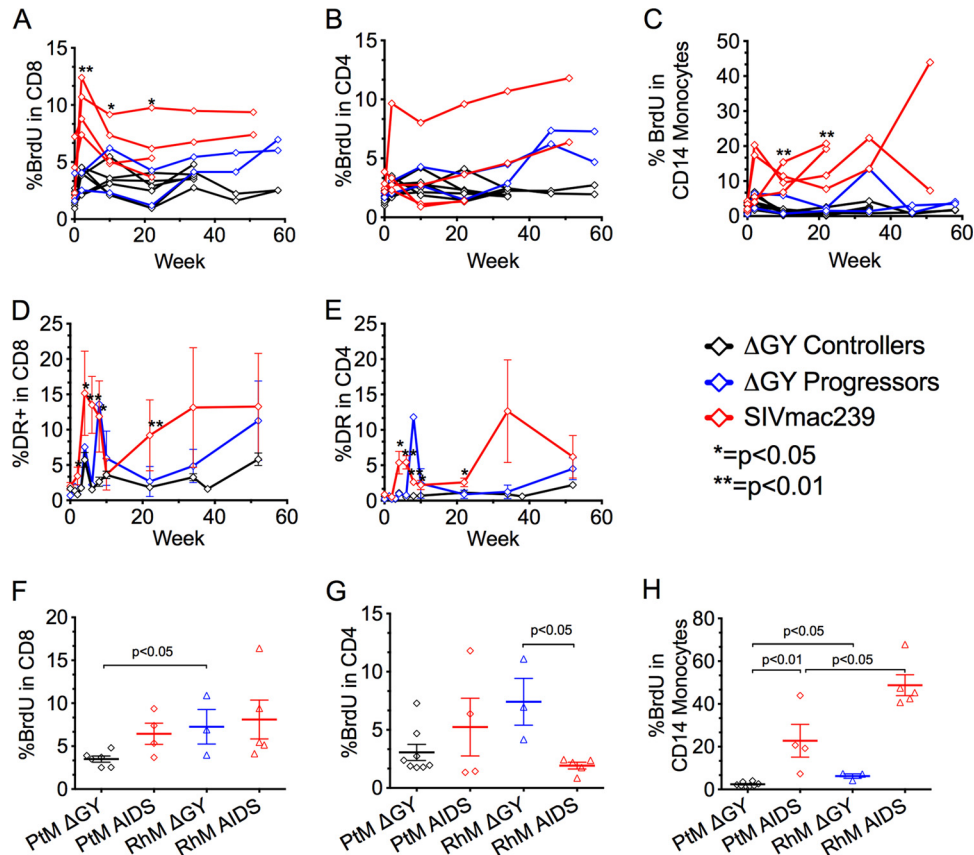


FIG 5 Lymphocyte turnover, monocyte turnover, and immune activation in SIV-infected macaques. (A to E) Immune activation in SIV-infected pig-tailed macaques was assessed by fluorescence-activated cell sorting (FACS) for BrdU incorporation to determine the percent turnover of CD8⁺ (A) and CD4⁺ (B) T cells and of CD14⁺ monocytes (C) and HLA-DR expression on CD8⁺ (D) and CD4⁺ (E) T cells. Values for Δ GY-infected controllers (black diamonds), Δ GY-infected progressors (blue diamonds), and SIVmac239-infected pig-tailed macaques (red diamonds) are shown. (F to H) Mean peak values (\pm SEM) for BrdU incorporation for CD4⁺ T cells (F), CD8⁺ T cells (G), and CD14⁺ monocytes (H) are compared between SIVmac239- and Δ GY-infected pig-tailed macaques and previously reported rhesus macaques (24). Values for SIVmac239-infected animals were determined at necropsy; values for Δ GY-infected animals were determined at week 22. Statistically significant differences are indicated. *P* values were determined using the Mann-Whitney nonparametric test.

that were at or below the limits of detection, this virus was clearly present and remained highly replication competent and susceptible to CD8⁺ cell control.

Neutralizing antibody responses to Δ GY. SIVmac239, from which Δ GY was derived, is highly resistant to neutralization and typically does not elicit high titers of neutralizing antibodies during infection (64). To determine if humoral immune responses were contributing to Δ GY control, neutralizing antibody titers to Δ GY were determined, as was the neutralization sensitivity of Δ GY relative to that of parental SIVmac239. Sera from 6 Δ GY-controlling pig-tailed macaques and the two Δ GY-infected animals that progressed to disease (GR26 and HA94) were evaluated prior to infection and at 28 and 46 weeks after infection. ID₅₀ values were determined for Δ GY as well as a panel of neutralization-sensitive (SIVmac251.6 and SIVsmE6602A5.VTRN) and neutralization-resistant (SIVsmE660.2A5 and SIVmac239) SIVs. As shown in Table 2, all animals generated high ID₅₀ titers to neutralization-sensitive SIVs, while no or extremely weak neutralization of SIVsmE660.2A5 or SIVmac239 was observed. Importantly, Δ GY-controlling macaques showed poor neutralization of Δ GY up to week 46, even though these animals controlled Δ GY by week 28. No differences were found in neutralization sensitivity

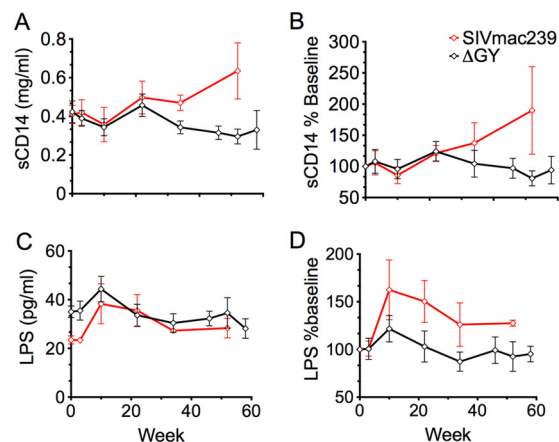


FIG 6 Microbial translocation of SIV-infected macaques. Plasma soluble CD14 (sCD14) and lipopolysaccharide (LPS) in pig-tailed macaques, as indicators of microbial translocation, are plotted over time (mean \pm SEM) for Δ GY-controlling (black diamonds) and SIVmac239-infected (red diamonds) pig-tailed macaques. (A) Levels of sCD14 remained at preinfection levels for Δ GY-infected controllers but increased over time with SIVmac239 infection. (C) LPS levels are shown for Δ GY-infected controllers and SIVmac239-infected animals. (B and D) Values are expressed as a percent change from preinfection levels and show trends for increases in SIVmac239 infection, although they are not statistically significant.

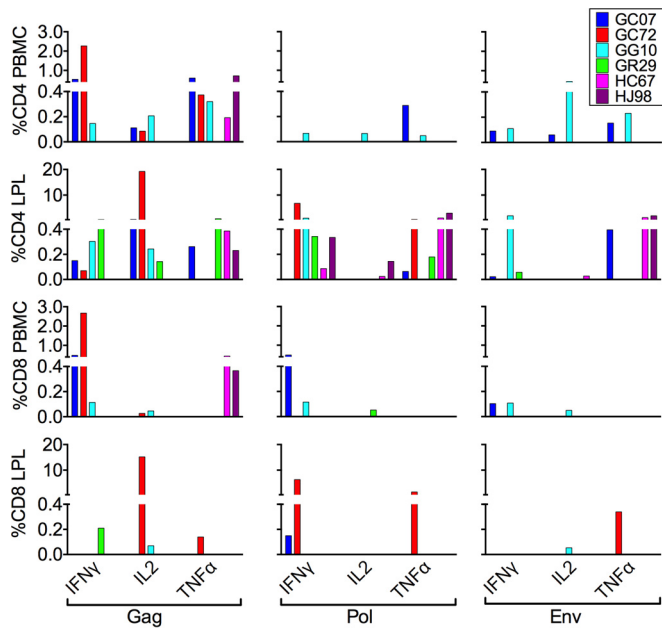


FIG 7 Intracellular cytokine responses against SIV Gag, Pol, and Env in CD4 and CD8 T lymphocytes from blood and gut during chronic Δ GY infection. Intracellular cytokine responses (IFN- γ , IL-2, and TNF- α) to SIV peptides (Gag, Pol, and Env) were measured in CD4⁺ and CD8⁺ T cells in peripheral blood (PBMCs) and small intestinal lamina propria in six Δ GY-controlling animals at week 66 after infection. The percentage of gated cells positive for a particular cytokine after stimulation with the relevant peptide pool are those that were $>0.05\%$ after subtracting the unstimulated control responses for each peptide pool. Animal identifiers are indicated at the top right.

between Δ GY and SIVmac239 when assayed using sera from SIVmac-infected rhesus macaques (not shown). Thus, Δ GY was not more neutralization sensitive than SIVmac239 and did not elicit autologous neutralizing titers during infection, indicating that neutralizing humoral immune responses were unlikely to have contributed to Δ GY control.

Viral evolution in Δ GY-infected progressing and controlling animals. To assess evolution of Δ GY in the two progressing pig-tailed macaques, both of which remained persistently viremic (see Fig. S1B in the supplemental material), single-genome amplification (SGA) and direct sequencing were performed on *env* genes isolated from plasma of GR26 at weeks 2, 6, 22, and 58 and from HA94 at week 76 (the time of necropsy) (see Fig. S2A in the supplemental material). Amino acid sequences of all amplicons from the cytoplasmic tail are shown in Fig. S2B and C in the supplemental material, and mutations occurring in $>10\%$ of amplicons for any individual time point are shown in Fig. 9A and summarized as a heat map in Fig. 9B. For GR26, the Δ GY mutation was maintained in all amplicons throughout infection. An R751G mutation, which is common *in vivo* in the parental SIVmac239 clone (65), was not detected at week 2 but was acquired in all amplicons by week 6 and maintained thereafter. Twelve additional mutations in the cytoplasmic tail appeared over time, although only one, an R722G mutation flanking the Δ GY mutation that first appeared at week 6, became fixed in 100% of amplicons by week 58. Although this change did not restore a Tyr-based GYxx \emptyset trafficking signal, it had been previously seen in 4 Δ GY-infected rhesus macaques that developed progressive disease and was proposed as a possible compensatory mutation (24). For animal HA94 at week 76, the

Δ GY mutation was maintained, and the R722G and R751G mutations were identified in all amplicons. Although mutations in this animal at positions 715 (A715T for HA94 and A715D for GR26) and 818 (T818I) were shared with GR26, mutations at positions 745 (T745I), 854 (E854G), and 879 (L879S) were unique, but none created a Tyr-based sorting motif (i.e., Yxx \emptyset).

As described above, in 4 pig-tailed macaques that controlled Δ GY to undetectable levels, CD8⁺ cell depletion led to a rapid reappearance of plasma viremia. SGA was performed on rebounding viruses in plasma from animals HC67 and HJ98 (CD8 depleted at week 82) to determine the extent of viral evolution during the prolonged period of elite host control (see Fig. S2A in the supplemental material). In contrast to the Δ GY-infected pig-tailed macaques with progressive infection, changes in the Env cytoplasmic tail in animal HC67 were minimal (Fig. 9B; see Fig. S2D in the supplemental material). The Δ GY mutation was retained in all 30 amplicons, and only a G860R mutation appeared in a minority (i.e., 4 of 30 amplicons). The R751G optimizing mutation was not found, consistent with rapid and durable control of Δ GY in this animal. Interestingly, following CD8 depletion in HJ98, the Δ GY mutation was maintained, and R722G and R751G were found in all amplicons, as was V837A (also seen in GR26) and a new mutation, S792L (Fig. 9B; see Fig. S2E in the supplemental material). Relative to that in HC67, viral control in HJ98 occurred more slowly in that the time to <100 RNA copies/ml was 20 weeks, compared to 8 weeks for HC67 (see Fig. S2A in the supplemental material). When SGA was performed on plasma RNA from HJ98 during its acute peak at week 2 (1.6×10^6 RNA copies/ml), the R722G mutation was found in 1 of 10 clones, suggesting that acquisition of this putative compensatory change contributed to the delay in Δ GY control in this animal.

We next sought to compare genetically the relative diversity over the entire Env protein for Δ GY-controlling and -progressing pig-tailed macaques and their divergence from the clonal viral inoculum. Amino acid highlighter plots for each animal show the positions of fixed mutations over time, underscoring the accumulation of mutations in the gp41 cytoplasmic domain in progressing animals (see Fig. S3A to D in the supplemental material). A nucleotide-based phylogenetic tree revealed 4 distinct lineages, representing each of the 4 infected macaques (Fig. 10A). The mean Env diversity and divergence from the parental clone were quantified by pairwise comparisons for each animal and represent the average accumulated changes that emerged after infection (Fig. 10B). Since viral sequences were obtained from samples originating from different weeks after infection, no direct comparisons were made, but it is clear that progressing animals, although sampled earlier after infection, had considerably more viral diversity and divergence, corresponding to the greater total replication in these animals than in controlling animals. This difference was substantial for GR26 at week 58 postinfection, with at least 7 times the diversity and nearly 3 times the divergence of viruses from either HJ98 or HC67 at week 82. For HA94, this difference was less, but it was still 3 times the diversity and nearly 2 times the divergence of controlling animals. For GR26, where longitudinal samples were analyzed, the means of both parameters increased over time in the context of poor early viral control. The endpoint means for diversity and divergence for both HJ98 and HC67 were more consistent with several weeks of infection, corresponding to acute viral replication and then immune control.

Taken together, these findings indicate that, relative to Δ GY-

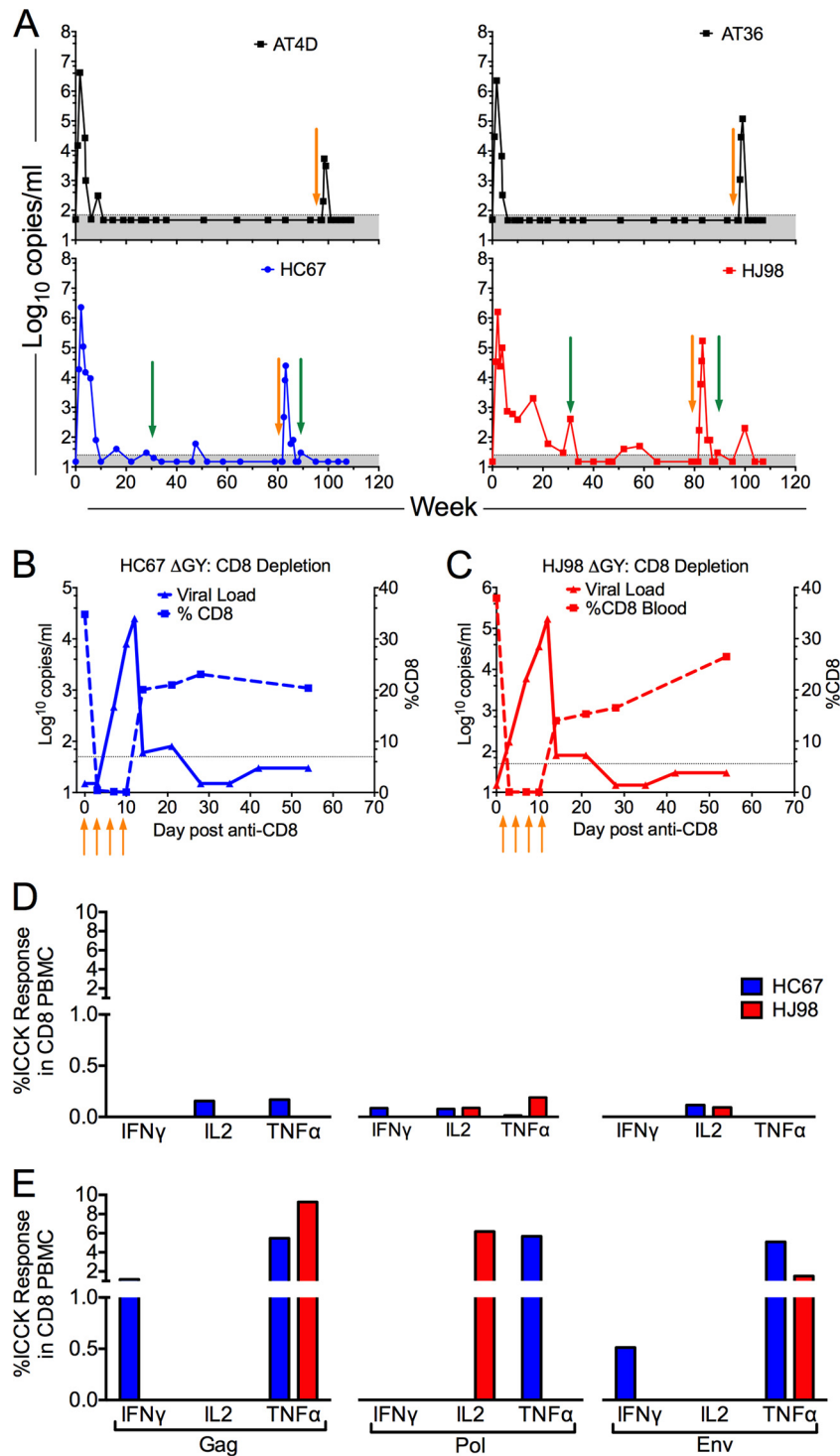


FIG 8 CD8⁺ cell depletion in Δ GY-controlling pig-tailed macaques. (A) Four Δ GY-controlling pig-tailed macaques (AT4D, AT36, HC67, and HJ98) underwent CD8⁺ cell depletion using monoclonal antibody cM-T807 or MT807R1, as described in Materials and Methods (orange arrows). Sampling times for determining intracellular cytokine responses to SIV peptides are indicated (green arrows). Following treatment, a transient burst of viral replication was observed in all four animals. Shaded areas indicate the limit of sensitivity for the plasma SIV RNA assay. (B and C) For HC67 and HJ98, graphs show the decline in peripheral CD8 T cells starting with the first of 4 anti-CD8 antibody injections. (D and E) Anti-SIV intracellular cytokine analyses (IFN- γ , IL-2, and TNF- α) for CD8⁺ T cell PBMCs at week 31 after Δ GY infection prior to CD8⁺ cell depletion (D) and at week 8 following CD8⁺ depletion (E).

TABLE 2 Neutralizing antibody responses in DGY-infected pig-tailed macaques

Δ GY group	Animal	Wk	ID ₅₀ ^a				
			Δ GY	SIVmac239	SIVsmE660-2A5	SIVsmE660-2A5.VTRN	SIVmac251.6
Controllers	GC07	Preinfection	<20	<20	<20	<30	<30
		28	<20	<20	<20	116,184	449,162
		46	25	<20	33	129,798	224,296
	GC72	Preinfection	<20	<20	<20	<30	<30
		28	<20	<20	<20	67,976	148,085
		46	<20	<20	<20	21,227	28,770
	GG10	Preinfection	<20	<20	<20	<30	<30
		28	<20	<20	<20	36,583	146,101
		46	<20	<20	<20	51,937	199,495
	GR29	Preinfection	<20	<20	<20	<30	32
		28	70	58	<20	20,807	195,239
		46	87	72	<20	9,578	118,720
	HC67	Preinfection	<20	<20	<20	<30	<30
		28	<20	<20	<20	>2,343,750	439,034
		46	<20	<20	46	>2,343,750	176,889
	HJ98	Preinfection	<20	<20	<20	<30	<30
		28	21	<20	<20	44,620	>2,343,750
		46	<20	<20	<20	579,940	324,247
Progressors	GR26	Preinfection	<20	<20	<20	<30	103
		28	30	<20	<20	>2,343,750	>2,343,750
		46	56	21	<20	>2,343,750	>2,343,750
	HA94	Preinfection	<20	<20	<20	<30	<30
		28	<20	<20	<20	44,620	408,428
		46	67	21	<20	579,940	>2,343,750

^a ID₅₀ values determined on TZM-bl cells for Δ GY-infected controlling and -progressing pig-tailed macaques using sera obtained before or at 28 or 46 weeks after infection. Neutralizing antibody responses of autologous sera to Δ GY and neutralization sensitivity of a panel of neutralization-sensitive and neutralization-resistant viruses are indicated. Neutralization-sensitive SIVsmE660-2A5.VTRN was generated by introducing 4 amino acid changes into neutralization-resistant SIVsmE660-2A5 (46).

infected pig-tailed macaques that progressed to disease, Δ GY control was associated with minimal viral replication and evolution. In Δ GY-progressing animals, amino acid changes were concentrated in regions of the V1/V2 and V4 variable loops and the gp41 ectodomain and frequently involved glycosylation sites, consistent with ongoing viral replication and immune escape, while only sporadic mutations occurred in these regions in Δ GY-controlling animals (see Fig. S3 in the supplemental material).

DISCUSSION

Pathogenic infections by CD4-tropic primate lentiviruses, HIV-1 in humans and SIV in Asian macaques, have in common the ability to rapidly infect and deplete CD4⁺ T cells in gut lymphoid tissue. An ensuing disruption in epithelial barrier function is associated with microbial translocation and chronic immune activation that contributes to generalized immune dysfunction, a loss of CD4⁺ T cell regenerative capacity, and an exhaustion of cellular responses (66). The host-pathogen relationship is further exacerbated in favor of the virus by a high mutation rate that enables HIV and SIV to escape from adaptive cellular and humoral immune responses (15, 67–73). Among SIV models, infection of pig-tailed macaques by diverse SIV isolates is a particularly robust model for disease, with animals typically progressing rapidly and uniformly to AIDS (8, 17, 18, 20). This more virulent outcome in pig-tailed macaques has been attributed to increased basal levels of immune activation resulting from compromised gut epithelial barrier function even in the absence of SIV infection (17, 20).

In the current report we show that relative to that of rhesus macaques, infection of pig-tailed macaques by Δ GY, an Env cyto-

plasmic domain mutant of SIVmac239 that lacks a conserved GYxxØ trafficking motif, paradoxically leads to markedly enhanced host control. We previously reported that in rhesus macaques, Δ GY replicates acutely to levels comparable to those for SIVmac239 but with the onset of host immune responses is suppressed to plasma levels 2 to 3 logs less than those for SIVmac239. Although gut CD4⁺ T cells were only transiently infected and there was no detectable microbial translocation, ongoing Δ GY replication occurred in rhesus macaques, associated with chronic immune activation, the appearance of possible compensatory mutations in the Env cytoplasmic tail, and progression to AIDS (24). In contrast, in pig-tailed macaques, Δ GY, although replicating acutely to levels identical to those for SIVmac239, was rapidly and profoundly controlled in the majority of animals to levels below the limit of detection. As in rhesus macaques (24), Δ GY largely spared CD4⁺ T cells in gut lamina propria and did not cause microbial translocation. However, in contrast to rhesus macaques, these animals did not have chronic immune activation, and they retained normal numbers of CD4⁺ T cells in gut and blood for up to 100 weeks after infection. Remarkably robust SIV-specific CD4⁺ T cell responses were generated and sustained in the intestine, although Δ GY persistence was demonstrated by anti-CD8 depletion at 82 to 97 weeks after infection. Given the high replication competence of Δ GY during acute infection and following CD8⁺ cell depletion, these findings indicate that this virus, while highly replication fit, was rendered susceptible to host immune control and that this control was more effective in pig-tailed than in rhesus macaques.

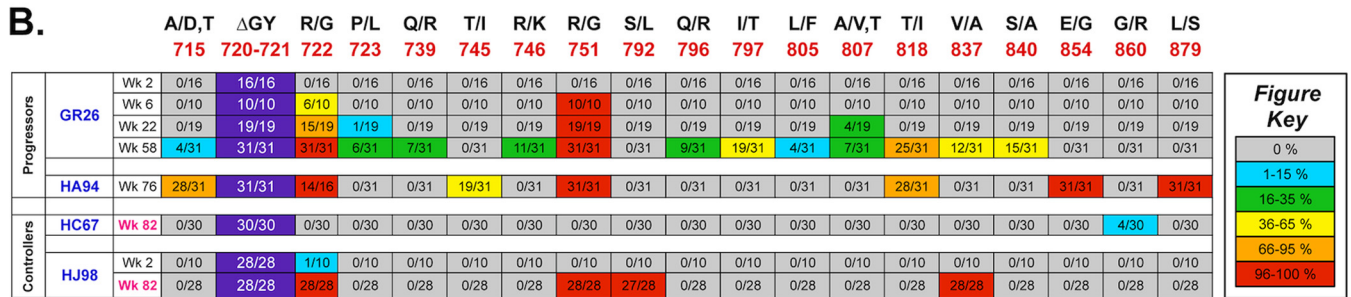
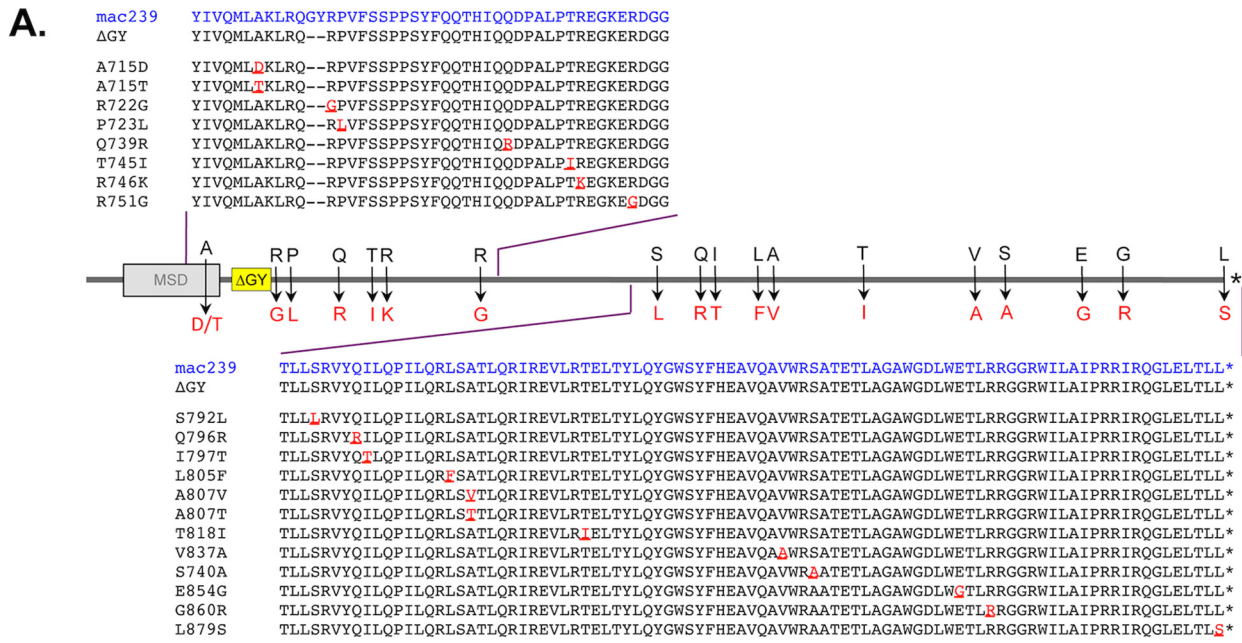


FIG 9 SGA analysis of ΔGY evolution in progressing and controlling pig-tailed macaques Single-genome amplification (SGA) of full-length *env* genes was performed at the indicated time points (Wk, week postinfection) on ΔGY-progressing (GR26 and HA94) and ΔGY-controlling (HC67 and HJ98) animals following CD8 depletion. (A) The diagram represents amino acid mutations and numbering (relative to SIVmac239) that appeared in >10% of amplicons for any time point in at least one animal. The position of the ΔGY deletion relative to the Env membrane-spanning domain (MSD) is shown. (B) The frequency of the indicated mutations in panel A relative to the number of amplicons is represented as a heat map with color codes for the proportion of sequences containing the mutation. The ΔGY deletion at positions 720 and 721 was retained in all amplicons. Specific mutations are discussed in the text. Results obtained following CD8 depletion (at week 82 for HC67 and HJ98) are indicated in red. Full amino acid sequences of all amplicons from the cytoplasmic domain are shown in Fig. S2B to E in the supplemental material.

A critical question is what host responses contribute to ΔGY's enhanced control. The rapid reappearance of virus following CD8⁺ cell depletion is consistent with control by cytotoxic T lymphocytes (CTL), a view supported by the prompt suppression of viremia during CD8⁺ T cell recovery and anamnestic antiviral cytokine responses. However, the anti-CD8α chain antibody used to deplete CD8⁺ cells is not specific for CTL (74, 75), and it is possible that virus control could have been exerted by CD8⁺ NK cells through antibody-dependent cell-mediated cytotoxicity (ADCC) or other cell types expressing this molecule. In addition, strong SIV-specific CD4⁺ T cell responses detected in blood and particularly in gut could have contributed, since in HIV infection these responses have been correlated with both enhanced antiviral CD8⁺ T cell activity and viral control (76–78). It is possible that sparing of CD4⁺ T cells in lamina propria during acute ΔGY infection enabled potent mucosal responses to occur. Although in humans and in macaques, control of HIV or SIV, respectively, has been correlated with particular MHC class I alleles (15, 54, 79, 80),

the high proportion (19 of 21 animals) of ΔGY-controlling pig-tailed macaques in this outbred population and the absence of any association between putative restrictive alleles and outcome suggests that non-HLA-dependent or multiple host immune effector mechanisms are involved. High titers of neutralizing antibodies to neutralization-sensitive SIVs were generated in ΔGY-infected pig-tailed macaques. However, these antibodies failed to neutralize ΔGY (Table 2), indicating that the ΔGY mutation neither rendered this virus more neutralization sensitive nor elicited more potent neutralizing antibodies. Taken together, our results indicate that the ΔGY mutation, while having no early effect on viral replicative capacity, rendered SIVmac239 highly susceptible to cellular control, with CD8⁺, CD4⁺, and possibly innate cellular responses playing a role (18, 81).

Transcriptomic profiling of SIV-infected pig-tailed macaques has revealed intense early proinflammatory and type I interferon responses in peripheral blood, lymph nodes, and gut that are sustained during chronic infection (18, 81). These responses are as-

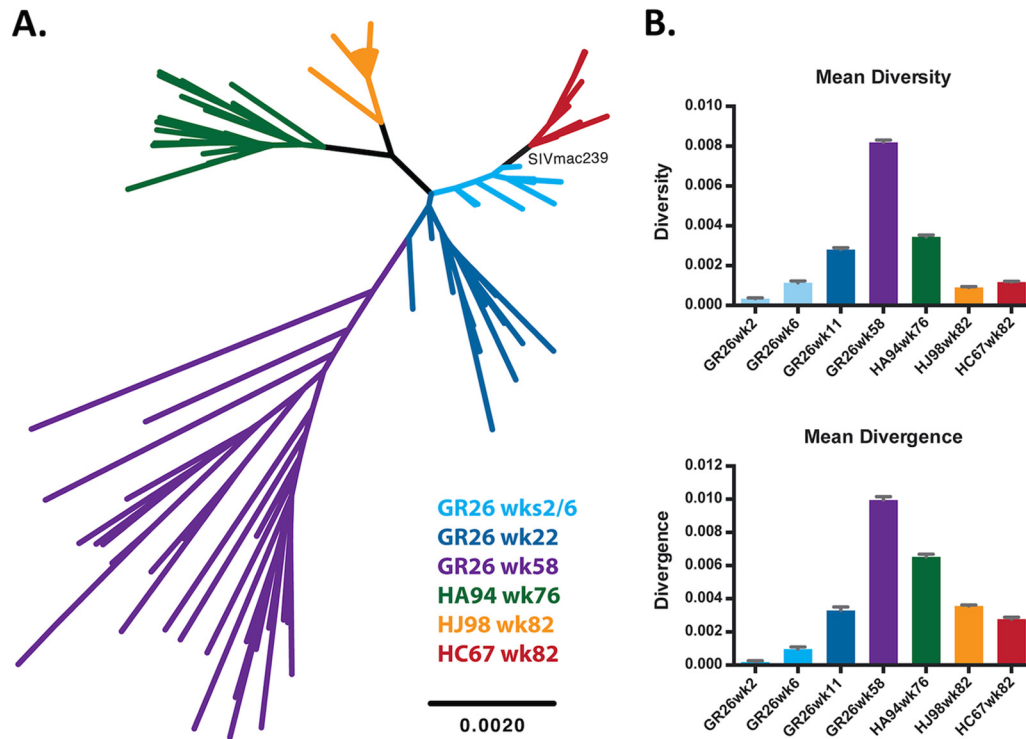


FIG 10 Single-genome amplification phylogenetic tree of Δ GY-progressing and Δ GY-controlling pig-tailed macaques. (A) Unrooted, neighbor-joining phylogenetic tree of *env* nucleotide sequences from Δ GY-infected pig-tailed macaques that progressed to disease (GR26 and HA94) and that controlled infection (HC67 and HJ98) following CD8 depletion. (B) Mean diversity and divergence were generated by pairwise comparisons within each animal, with error bars representing SEM. All branches and bar graphs are color coded to the legend key, with weeks after infection indicated.

sociated with DNA damage pathways, T and B cell proliferation, apoptosis, and signatures of innate immune activation that are in marked contrast to those in natural hosts of SIV, which mount acute responses that are often greater than those seen in macaques but are uniformly downregulated during chronic infection (82, 83). Although a similar spectrum of responses occurs in SIVmac-infected rhesus macaques (40, 81), accelerated or more robust responses may occur in pig-tailed macaques, which could account for Δ GY's rapid control in this species. Although Δ GY-controlling pig-tailed macaques resemble natural hosts of SIV in remaining clinically well with normal levels of CD4⁺ T cells in blood and gut and no systemic immune activation, natural hosts tolerate high levels of viremia following downregulation of their acute immune responses, while Δ GY-infected pig-tailed macaques exhibit a high degree of viral control (84). Further studies of the transcriptomic responses of pig-tailed macaques during acute and chronic Δ GY infection, along with a longitudinal assessment of their host immune response, will provide a valuable probe to assess the magnitude and breadth of host responses that correlate with Δ GY control and the extent to which these responses persist during chronic infection.

It remains to be determined how the Gly-720/Tyr-721 amino acid deletion within the GYxxØ trafficking motif renders SIVmac more susceptible to control in pig-tailed macaques. A YxxØ motif within 6 or 7 amino acids of the predicted membrane spanning domain is universally conserved in all primate lentiviruses and, in association with a proximal glycine, mediates binding to cellular clathrin adaptor complexes and highly efficient clathrin-dependent endocytosis of Env from the plasma membrane (85–90). Al-

though for HIV and SIV, additional endocytic signals exist (85–87, 91), loss of this most membrane-proximal motif by the Δ GY mutation has been associated with modest increases in Env expression on the plasma membrane (85). It is possible that such an increase could enhance the susceptibility of virus-producing cells to ADCC (91). In addition to the AP2 endocytic adaptor complex, this GYxxØ domain also binds to the AP1 complex (87, 89), and alterations in intracellular trafficking in biosynthetic pathways from the Golgi apparatus or postendocytic sorting of Env from endosomes could alter Env processing or its loading and presentation on MHC class I or II molecules to increase target cell susceptibility to immune attack or the priming of cellular responses by antigen-presenting cells (92–94).

The Δ GY mutation does not affect CD4 or CCR5 tropism in standard cell-cell fusion assays (95) (not shown). However, a less well-defined region that overlaps the GYxxØ motif is a potent basolateral sorting signal (96–99). It is possible that alteration of this directional signal for viral assembly could affect viral budding or cell-to-cell spread in specific anatomical compartments. Alternatively, mucosal tissues are known to express abundant proinflammatory and interferon-stimulated genes (5, 100), and a suppression of Δ GY replication at this site could have occurred had the Δ GY mutation rendered SIVmac239 more susceptible to these responses.

One intriguing and striking alteration associated with the Δ GY mutation was a marked reduction in infected macrophages, as determined by *in situ* hybridization and multilabel confocal microscopy. This finding correlated with the absence of detectable virus in the central nervous system (CNS), where monocyte/mac-

rophage trafficking of infected cells is thought to play a critical role in neuro-AIDS (101, 102). Δ GY-infected animals also exhibited a lack of BrdU incorporation in monocytes during chronic infection, which we have shown correlates with macrophage turnover and progression to AIDS (34). While there has been recent controversy as to whether myeloid cells isolated from tissues are actually infected or have simply phagocytosed debris from neighboring SIV-infected T cells (103), previous analyses of tissues from SIV-infected macaques (24, 35, 101, 104, 105) and the current study show SIV antigens and nucleic acids in tissues from SIVmac239-infected pig-tailed macaques, which were distinguishable from phagocytosed SIV antigens and CD3⁺ T cell fragments (Fig. 3). Although it is unclear how the Δ GY mutation led to this outcome, macrophages express a number of interferon-stimulated genes, including SAMHD1 (106) and IFITM family members (107), and it is possible that the Δ GY mutation rendered this virus more susceptible to these or other cellular factors expressed in macrophages.

Two Δ GY-infected pig-tailed macaques (GR26 and HA94) developed persisting viremia and progressed to disease by 74 and 76 weeks. Although their disease was atypical for AIDS in that CD4⁺ T cells in blood and lamina propria were only mildly depleted (Fig. 2) and macrophages were not clearly infected, both animals developed chronic immune activation, as reflected in BrdU incorporation in CD4⁺ and CD8⁺ T cells and HLA-DR expression on CD8⁺ T cells. These animals also developed thrombocytopenia, which is commonly associated with SIV disease progression in pig-tailed macaques (108), and tissues at necropsy showed pulmonary arteriopathy uniquely associated with SIV infection (56–58). Single-genome amplification of the Env cytoplasmic domain in both animals showed conservation of the Δ GY mutation, as well as R751G, which is a well-described mutation for the SIVmac239 clone (65). Of particular interest were novel mutations that likely reflected selection pressure to restore defects caused by the Δ GY mutation (Fig. 9). Among these, an R722G mutation flanking the Δ GY mutation became fixed in all amplicons at necropsy in both animals. In GR26, R722G was not present during peak viremia at week 2 but was detectable in 6 of 10 amplicons at week 6, suggesting that any role it played in fitness occurred after the onset of host immune responses and the decline in viremia. Although this change did not create a recognizable Tyr-based trafficking motif, it was also noted in at least some amplicons in all 4 rhesus macaques that progressed to AIDS (24). Two changes seen previously in rhesus macaques, an S727P mutation, which in small numbers of rhesus macaques partially restored gut tropism and pathogenicity to Δ GY (28), and a deletion of QTH from amino acid positions 734 to 736, were not observed in Δ GY-progressing pig-tailed macaques. Although additional changes were seen (Fig. 9), these were largely nonoverlapping, with the exception of a conservative T818I mutation in 80 to 90% of amplicons. Given the possibility that some or all of these mutations could be compensating for a defect caused by the GY deletion, assessing their impact on the Δ GY virus *in vitro* and *in vivo* should provide an approach to probe the virological determinants for Δ GY's altered tropism and enhanced susceptibility to host control.

Although Δ GY viremia was suppressed below the limits of detection in the majority of pig-tailed macaques, viral persistence was clearly demonstrated by anti-CD8 depletion (Fig. 8). This finding raises intriguing questions concerning the cellular and anatomic reservoirs that harbored this virus and whether there was

ongoing viral evolution in these sites. As demonstrated by Δ GY's robust acute replication and rapid kinetics of rebound following CD8⁺ cell depletion, this virus remained highly replication fit despite strong host control. For HIV-1, viral persistence continues during antiretroviral therapy, since viremia recurs following cessation of therapy even after years of suppression (109, 110). It remains controversial whether HIV-1 that emerges in this setting is truly latent or if low levels of replication and evolution continue during therapy (111, 112). When SGA was performed following CD8⁺ depletion on two Δ GY-infected animals that had maintained low to undetectable levels of viremia for several months, there was markedly less divergence and diversity than in animals that progressed to disease (Fig. 10). For HC67, which controlled plasma viremia by 10 weeks, little to no evolution occurred in the Env cytoplasmic domain. Moreover, the absence of the R751G fitness mutation likely indicated that rapid and potent viral suppression occurred and was maintained. In contrast, for HJ98, which did not control Δ GY viremia until 20 weeks postinfection, mutations present following CD8 depletion included both R751G and R722G. The latter mutation, previously implicated in Δ GY-infected rhesus macaques as a possible compensatory mutation (24), was also present in 1 of 10 amplicons at the peak of acute viremia, suggesting that it may have delayed host control. It remains unclear if the additional changes acquired in virus from HJ98 occurred during this delayed period of control or during the aviremic period that followed. However, the paucity of changes in gp120 and the gp41 ectodomain for both HC67 and HJ98 is in marked contrast to the number of changes in viruses identified in Δ GY-progressing animals (see Fig. S3 in the supplemental material) and suggests that there was little viral turnover in these animals following control. Given intense interest in the cells and anatomic compartments where HIV and SIV reservoirs reside and in their susceptibility to pharmacological (113, 114) and immunological (115) interventions, the Δ GY model of host control in pig-tailed macaques could provide an opportunity to explore novel approaches to eradicate virus that persists in the face of immune responses that control but do not eradicate infection.

In summary, deletion of Gly-720 and Tyr-721 from the conserved GYxxØ (GYRPV) trafficking motif in the SIVmac239 Env cytoplasmic domain results in a novel phenotype in pig-tailed macaques in which this virus replicates to wild-type levels during acute infection, spares mucosal CD4⁺ T cells and macrophages, and is rapidly and profoundly controlled in the absence of chronic immune activation. The finding that elite control of Δ GY paradoxically is seen in pig-tail macaques, a species that progresses more rapidly to AIDS following SIV infection, suggests that the Δ GY mutation has rendered SIVmac highly susceptible to immune responses in this species. A critical future question will be to determine whether immune responses that are effective in controlling Δ GY will enable pig-tailed macaques to resist pathogenic challenge viruses. Although the SIV Δ Nef model, in which SIVmac239 is attenuated by deletion of its *nef* gene, remains the best model for protection from homologous SIV challenges (116–118), Δ Nef provides less effective protection from heterologous SIV or simian-human immunodeficiency virus (SHIV) challenges (119–121). Studies in pig-tailed macaques that assess the ability of Δ GY infection to elicit protective immune responses are in progress. As a model in which a highly replication-fit but immunologically controllable virus has been generated by only a 2-amino-acid deletion in a cellular trafficking signal, the Δ GY/pig-tailed

macaque model will provide an opportunity to elucidate viral, cellular, and host factors that are critical determinants in the delicate balance between viral persistence, host control, and progression to AIDS.

ACKNOWLEDGMENTS

At the Tulane National Primate Research Center (TNPRC), we thank Lara Doyle for veterinary support, Julie Bruhn and Calvin Lanclos for flow cytometry support, David Liu and Peter Didier for pathology support, Robin Rodriguez for image preparation, and Maury Duplantier for tissue collection. At the University of Alabama, we thank Jackie Stallworth for excellent technical assistance. MHC genotyping assistance was provided by Patrick Bohn and the WNPRC Genetics Services Unit.

REFERENCES

- Marchetti G, Tincati C, Silvestri G. 2013. Microbial translocation in the pathogenesis of HIV infection and AIDS. *Clin Microbiol Rev* 26:2–18. <http://dx.doi.org/10.1128/CMR.00050-12>.
- Klatt NR, Chomont N, Douek DC, Deeks SG. 2013. Immune activation and HIV persistence: implications for curative approaches to HIV infection. *Immunol Rev* 254:326–342. <http://dx.doi.org/10.1111/imr.12065>.
- Estes JD. 2012. Enhancing immune responses to limit chronic immune activation during SIV. *J Clin Invest* 122:1611–1614. <http://dx.doi.org/10.1172/JCI63389>.
- Reeves RK, Evans TI, Gillis J, Wong FE, Kang G, Li Q, Johnson RP. 2012. SIV infection induces accumulation of plasmacytoid dendritic cells in the gut mucosa. *J Infect Dis* 206:1462–1468. <http://dx.doi.org/10.1093/infdis/jis408>.
- Estes JD, Harris LD, Klatt NR, Tabb B, Pittaluga S, Paiardini M, Barclay GR, Smedley J, Pung R, Oliveira KM, Hirsch VM, Silvestri G, Douek DC, Miller CJ, Haase AT, Lifson J, Brechley JM. 2010. Damaged intestinal epithelial integrity linked to microbial translocation in pathogenic simian immunodeficiency virus infections. *PLoS Pathog* 6:e1001052. <http://dx.doi.org/10.1371/journal.ppat.1001052>.
- Wijewardana V, Kristoff J, Xu C, Ma D, Haret-Richter G, Stock JL, Policicchio BB, Mobley AD, Nusbaum R, Aamer H, Trichel A, Ribeiro RM, Apetrei C, Pandrea I. 2013. Kinetics of myeloid dendritic cell trafficking and activation: impact on progressive, nonprogressive and controlled SIV infections. *PLoS Pathog* 9:e1003600. <http://dx.doi.org/10.1371/journal.ppat.1003600>.
- Fraser C, Lythgoe K, Leventhal GE, Shirreff G, Hollingsworth TD, Alison S, Bonhoeffer S. 2014. Virulence and pathogenesis of HIV-1 infection: an evolutionary perspective. *Science* 343:1243727. <http://dx.doi.org/10.1126/science.1243727>.
- Goldstein S, Ourmanov I, Brown CR, Plishka R, Buckler-White A, Byrum R, Hirsch VM. 2005. Plateau levels of viremia correlate with the degree of CD4⁺-T-cell loss in simian immunodeficiency virus SIVagm-infected pigtailed macaques: variable pathogenicity of natural SIVagm isolates. *J Virol* 79:5153–5162. <http://dx.doi.org/10.1128/JVI.79.8.5153-5162.2005>.
- Pandrea I, Gautam R, Ribeiro RM, Brechley JM, Butler IF, Pattison M, Rasmussen T, Marx PA, Silvestri G, Lackner AA, Perelson AS, Douek DC, Veazey RS, Apetrei C. 2007. Acute loss of intestinal CD4⁺ T cells in not predictive of simian immunodeficiency virus virulence. *J Immunol* 179:3035–3046. <http://dx.doi.org/10.4049/jimmunol.179.5.3035>.
- Chahroudi A, Bosinger SE, Vanderford TH, Paiardini M, Silvestri G. 2012. Natural SIV hosts: showing AIDS the door. *Science* 335:1188–1193. <http://dx.doi.org/10.1126/science.1217550>.
- Milush JM, Mir KD, Sundaravaran V, Gordon SN, Engram J, Cano CA, Reeves JD, Anton E, O'Neill E, Butler E, Hancock K, Cole KS, Brechley JM, Else JG, Silvestri G, Sodora DL. 2011. Lack of clinical AIDS in SIV-infected sooty mangabeys with significant CD4⁺ T cell loss is associated with double-negative T cells. *J Clin Invest* 121:1102–1110. <http://dx.doi.org/10.1172/JCI44876>.
- Ling B, Veazey RS, Luckay A, Penedo C, Xu K, Lifson JD, Marx PA. 2002. SIV(mac) pathogenesis in rhesus macaques of Chinese and Indian origin compared with primary HIV infections in humans. *AIDS* 16:1489–1496. <http://dx.doi.org/10.1097/00002030-200207260-00005>.
- Ling B, Mohan M, Lackner AA, Green LC, Marx PA, Doyle LA, Veazey RS. 2010. The large intestine as a major reservoir for simian immunodeficiency virus in macaques with long-term, nonprogressing infection. *J Infect Dis* 202:1846–1854. <http://dx.doi.org/10.1086/657413>.
- Ling B, Veazey RS, Hart M, Lackner AA, Kuroda M, Pahar B, Marx PA. 2007. Early restoration of mucosal CD4 memory CCR5 T cells in the gut of SIV-infected rhesus predicts long term non-progression. *AIDS* 21:2377–2385. <http://dx.doi.org/10.1097/QAD.0b013e3282f08b32>.
- Goulder PJ, Watkins DI. 2008. Impact of MHC class I diversity on immune control of immunodeficiency virus replication. *Nat Rev Immunol* 8:619–630. <http://dx.doi.org/10.1038/nri2357>.
- Loffredo JT, Maxwell J, Qi Y, Glidden CE, Borchardt GJ, Soma T, Bean AT, Beal DR, Wilson NA, Rehauer WM, Lifson JD, Carrington M, Watkins DI. 2007. Mamu-B*08-positive macaques control simian immunodeficiency virus replication. *J Virol* 81:8827–8832. <http://dx.doi.org/10.1128/JVI.00895-07>.
- Klatt NR, Canary LA, Vanderford TH, Vinton CL, Engram JC, Dunham RM, Cronise HE, Swerczek JM, Lafont BA, Picker LJ, Silvestri G, Brechley JM. 2012. Dynamics of simian immunodeficiency virus SIVmac239 infection in pigtail macaques. *J Virol* 86:1203–1213. <http://dx.doi.org/10.1128/JVI.06033-11>.
- Lederer S, Favre D, Walters KA, Proll S, Kanwar B, Kasakow Z, Baskin CR, Palermo R, McCune JM, Katze MG. 2009. Transcriptional profiling in pathogenic and non-pathogenic SIV infections reveals significant distinctions in kinetics and tissue compartmentalization. *PLoS Pathog* 5:e1000296. <http://dx.doi.org/10.1371/journal.ppat.1000296>.
- Pandrea I, Gauvin T, Gautam R, Kristoff J, Mandell D, Montefiori D, Keele BF, Ribeiro RM, Veazey RS, Apetrei C. 2011. Functional cure of SIVagm infection in rhesus macaques results in complete recovery of CD4⁺ T cells and is reverted by CD8⁺ cell depletion. *PLoS Pathog* 7:e1002170. <http://dx.doi.org/10.1371/journal.ppat.1002170>.
- Canary LA, Vinton CL, Morcock DR, Pierce JB, Estes JD, Brechley JM, Klatt NR. 2013. Rate of AIDS progression is associated with gastrointestinal dysfunction in simian immunodeficiency virus-infected pigtail macaques. *J Immunol* 190:2959–2965. <http://dx.doi.org/10.4049/jimmunol.1202319>.
- Klatt NR, Harris LD, Vinton CL, Sung H, Briant JA, Tabb B, Morcock D, McGinty JW, Lifson JD, Lafont BA, Martin MA, Levine AD, Estes JD, Brechley JM. 2010. Compromised gastrointestinal integrity in pigtail macaques is associated with increased microbial translocation, immune activation, and IL-17 production in the absence of SIV infection. *Mucosal Immunol* 3:387–398. <http://dx.doi.org/10.1038/mi.2010.14>.
- Brennan G, Kozyrev Y, Hu SL. 2008. TRIMCyp expression in Old World primates *Macaca nemestrina* and *Macaca fascicularis*. *Proc Natl Acad Sci U S A* 105:3569–3574. <http://dx.doi.org/10.1073/pnas.0709511105>.
- Wu F, Kirmaier A, Goeken R, Ourmanov I, Hall L, Morgan JS, Matsuda K, Buckler-White A, Tomioka K, Plishka R, Whitted S, Johnson W, Hirsch VM. 2013. TRIM5 alpha drives SIVsmm evolution in rhesus macaques. *PLoS Pathog* 9:e1003577. <http://dx.doi.org/10.1371/journal.ppat.1003577>.
- Breed MW, Jordan AP, Aye PP, Lichtveld CF, Midkiff CC, Schiro FR, Haggarty BS, Sugimoto C, Alvarez X, Sandler NG, Douek DC, Kuroda MJ, Pahar B, Piatak M, Jr, Lifson JD, Keele BF, Hoxie JA, Lackner AA. 2013. Loss of a tyrosine-dependent trafficking motif in the simian immunodeficiency virus envelope cytoplasmic tail spares mucosal CD4 cells but does not prevent disease progression. *J Virol* 87:1528–1543. <http://dx.doi.org/10.1128/JVI.01928-12>.
- Fultz PN, Vance PJ, Endres MJ, Tao B, Dvorin JD, Davis IC, Lifson JD, Montefiori DC, Marsh M, Malim MH, Hoxie JA. 2001. In vivo attenuation of simian immunodeficiency virus by disruption of a tyrosine-dependent sorting signal in the envelope glycoprotein cytoplasmic tail. *J Virol* 75:278–291. <http://dx.doi.org/10.1128/JVI.75.1.278-291.2001>.
- Mattapallil JJ, Douek DC, Hill B, Nishimura Y, Martin M, Roederer M. 2005. Massive infection and loss of memory CD4⁺ T cells in multiple tissues during acute SIV infection. *Nature* 434:1093–1097. <http://dx.doi.org/10.1038/nature03501>.
- Veazey RS, DeMaria M, Chalifoux LV, Shvets DE, Pauley DR, Knight HL, Rosenzweig M, Johnson RP, Desrosiers RC, Lackner AA. 1998. Gastrointestinal tract as a major site of CD4⁺ T cell depletion and viral replication in SIV infection. *Science* 280:427–431. <http://dx.doi.org/10.1126/science.280.5362.427>.
- Breed MW, Jordan AP, Aye PP, Sugimoto C, Alvarez X, Kuroda MJ,

- Pahar B, Keele BF, Hoxie JA, Lackner AA. 2013. A single amino acid mutation in the envelope cytoplasmic tail restores the ability of an attenuated simian immunodeficiency virus mutant to deplete mucosal CD4+ T cells. *J Virol* 87:13048–13052. <http://dx.doi.org/10.1128/JVI.02126-13>.
29. National Research Council. 2011. Guide for the care and use of laboratory animals, 8th ed. National Academies Press, Washington, DC.
30. Cline AN, Bess JW, Piatak M, Jr, Lifson JD. 2005. Highly sensitive SIV plasma viral load assay: practical considerations, realistic performance expectations, and application to reverse engineering of vaccines for AIDS. *J Med Primatol* 34:303–312. <http://dx.doi.org/10.1111/j.1600-0684.2005.00128.x>.
31. Wang X, Das A, Lackner AA, Veazey RS, Pahar B. 2008. Intestinal double positive CD4+CD8+ T cells of neonatal rhesus macaques are proliferating, activated, memory cells and primary targets for SIVMAC251 infection. *Blood* 112:4981–4990. <http://dx.doi.org/10.1182/blood-2008-05-160077>.
32. Veazey RS, Lifson J, Pandrea I, Purcell J, Piatak M, Lackner AA. 2003. Simian immunodeficiency virus (SIV) infection in neonatal macaques. *J Virol* 77:8783–8792. <http://dx.doi.org/10.1128/JVI.77.16.8783-8792.2003>.
33. Pahar B, Cantu MA, Zhao W, Kuroda MJ, Veazey RS, Montefiori DC, Clements JD, Aye PP, Lackner AA, Lovgren-Bengtsson K, Sestak K. 2006. Single epitope mucosal vaccine delivered via immuno-stimulating complexes induces low level of immunity against simian-HIV. *Vaccine* 24:6839–6849. <http://dx.doi.org/10.1016/j.vaccine.2006.06.050>.
34. Hasegawa A, Liu H, Ling B, Borda JT, Alvarez X, Sugimoto C, Vinet-Oliphant H, Kim WK, Williams KC, Ribeiro RM, Lackner AA, Veazey RS, Kuroda MJ. 2009. The level of monocyte turnover predicts disease progression in the macaque model of AIDS. *Blood* 114:2917–2925. <http://dx.doi.org/10.1182/blood-2009-02-204263>.
35. Burdo TH, Soulas C, Orzechowski K, Button J, Krishnan A, Sugimoto C, Alvarez X, Kuroda MJ, Williams KC. 2010. Increased monocyte turnover from bone marrow correlates with severity of SIV encephalitis and CD163 levels in plasma. *PLoS Pathog* 6:e1000842. <http://dx.doi.org/10.1371/journal.ppat.1000842>.
36. Pahar B, Wang X, Dufour J, Lackner AA, Veazey RS. 2007. Virus-specific T cell responses in macaques acutely infected with SHIV(sf162p3). *Virology* 363:36–47. <http://dx.doi.org/10.1016/j.viro.2007.01.010>.
37. Faul EJ, Aye PP, Papaneri AB, Pahar B, McGettigan JP, Schiro F, Chervoneva I, Montefiori DC, Lackner AA, Schnell MJ. 2009. Rabies virus-based vaccines elicit neutralizing antibodies, poly-functional CD8+ T cell, and protect rhesus macaques from AIDS-like disease after SIV(mac251) challenge. *Vaccine* 28:299–308. <http://dx.doi.org/10.1016/j.vaccine.2009.10.051>.
38. Brechley JM, Price DA, Schacker TW, Asher TE, Silvestri G, Rao S, Kazzaz Z, Bornstein E, Lambotte O, Altmann D, Blazar BR, Rodriguez B, Teixeira-Johnson L, Landay A, Martin JN, Hecht FM, Picker LJ, Lederman MM, Deeks SG, Douek DC. 2006. Microbial translocation is a cause of systemic immune activation in chronic HIV infection. *Nat Med* 12:1365–1371.
39. Sandler NG, Wand H, Roque A, Law M, Nason MC, Nixon DE, Pedersen C, Ruxrungtham K, Lewin SR, Emery S, Neaton JD, Brechley JM, Deeks SG, Sereti I, Douek DC. 2011. Plasma levels of soluble CD14 independently predict mortality in HIV infection. *J Infect Dis* 203:780–790. <http://dx.doi.org/10.1093/infdis/jiq118>.
40. Rotger M, Dalmau J, Rauch A, McLaren P, Bosinger SE, Martinez R, Sandler NG, Roque A, Liebner J, Battagay M, Bernasconi E, Descombes P, Erkizia I, Fellay J, Hirschel B, Miro JM, Palou E, Hoffmann M, Massanella M, Blanco J, Woods M, Gunthard HF, de Bakker P, Douek DC, Silvestri G, Martinez-Picado J, Telenti A. 2011. Comparative transcriptomics of extreme phenotypes of human HIV-1 infection and SIV infection in sooty mangabey and rhesus macaque. *J Clin Invest* 121:2391–2400. <http://dx.doi.org/10.1172/JCI45235>.
41. Gooneratne SL, Alinejad-Rokny H, Ebrahimi D, Bohn PS, Wiseman RW, O'Connor DH, Davenport MP, Kent SJ. 2014. Linking pig-tailed macaque major histocompatibility complex class I haplotypes and cytotoxic T lymphocyte escape mutations in simian immunodeficiency virus infection. *J Virol* 88:14310–14325. <http://dx.doi.org/10.1128/JVI.02428-14>.
42. Karl JA, Bohn PS, Wiseman RW, Nimityongskul FA, Lank SM, Starrett GJ, O'Connor DH. 2013. Major histocompatibility complex class I haplotype diversity in Chinese rhesus macaques. *G3 (Bethesda)* 3:1195–1201. <http://dx.doi.org/10.1534/g3.113.006254>.
43. Wiseman RW, Karl JA, Bohn PS, Nimityongskul FA, Starrett GJ, O'Connor DH. 2013. Haplessly hoping: macaque major histocompatibility complex made easy. *ILAR J* 54:196–210. <http://dx.doi.org/10.1093/ilar/ilt036>.
44. Montefiori DC. 2005. Evaluating neutralizing antibodies against HIV, SIV, and SHIV in luciferase reporter gene assays. *Curr Protoc Immunol* Chapter 12:Unit 12.11.
45. Gandhi RT, Walker BD. 2002. Immunologic control of HIV-1. *Annu Rev Med* 53:149–172. <http://dx.doi.org/10.1146/annurev.med.53.082901.104011>.
46. Roederer W, Keele BF, Schmidt SD, Mason RD, Welles HC, Fischer W, Labranche C, Foulds KE, Louder MK, Yang ZY, Todd JP, Buzby AP, Mach LV, Shen L, Seaton KE, Ward BM, Bailer RT, Gottardo R, Gu W, Ferrari G, Alam SM, Denny TN, Montefiori DC, Tomaras GD, Korber BT, Nason MC, Seder RA, Koup RA, Letvin NL, Rao SS, Nabel GJ, Mascola JR. 2014. Immunological and virological mechanisms of vaccine-mediated protection against SIV and HIV. *Nature* 505:502–508. <http://dx.doi.org/10.1038/nature12893>.
47. Vinet-Oliphant H, Alvarez X, Buza E, Borda JT, Mohan M, Aye PP, Tuluc F, Douglas SD, Lackner AA. 2010. Neurokinin-1 receptor (NK1-R) expression in the brains of SIV-infected rhesus macaques: implications for substance P in NK1-R immune cell trafficking into the CNS. *Am J Pathol* 177:1286–1297. <http://dx.doi.org/10.2353/ajpath.2010.091109>.
48. Wang X, Rasmussen T, Pahar B, Poonia B, Alvarez X, Lackner AA, Veazey RS. 2007. Massive infection and loss of CD4+ T cells occurs in the intestinal tract of neonatal rhesus macaques in acute SIV infection. *Blood* 109:1174–1181.
49. Brechley JM, Vinton C, Tabb B, Hao XP, Connick E, Paiardini M, Lifson JD, Silvestri G, Estes JD. 2012. Differential infection patterns of CD4+ T cells and lymphoid tissue viral burden distinguish progressive and nonprogressive lentiviral infections. *Blood* 120:4172–4181. <http://dx.doi.org/10.1182/blood-2012-06-437608>.
50. Wang X, Pahar B, Rasmussen T, Alvarez X, Dufour J, Rasmussen K, Lackner AA, Veazey RS. 2008. Differential cross-reactivity of monoclonal antibody OPD4 (anti-CD45RO) in macaques. *Dev Comp Immunol* 32:859–868. <http://dx.doi.org/10.1016/j.dci.2007.12.009>.
51. Cai Y, Sugimoto C, Arainga M, Alvarez X, Didier ES, Kuroda MJ. 2014. In vivo characterization of alveolar and interstitial lung macrophages in rhesus macaques: implications for understanding lung disease in humans. *J Immunol* 192:2821–2829. <http://dx.doi.org/10.4049/jimmunol.1302269>.
52. Keele BF, Li H, Learn GH, Hraber P, Giorgi EE, Grayson T, Sun C, Chen Y, Yeh WW, Letvin NL, Mascola JR, Nabel GJ, Haynes BF, Bhattacharya T, Perelson AS, Korber BT, Hahn BH, Shaw GM. 2009. Low-dose rectal inoculation of rhesus macaques by SIVsmE660 or SIVmac251 recapitulates human mucosal infection by HIV-1. *J Exp Med* 206:1117–1134. <http://dx.doi.org/10.1084/jem.20082831>.
53. Deng W, Maust BS, Nickle DC, Learn GH, Liu Y, Heath L, Kosakovsky Pond SL, Mullins JL. 2010. DIVEIN: a web server to analyze phylogenies, sequence divergence, diversity, and informative sites. *Biotechniques* 48:405–408. <http://dx.doi.org/10.2144/000113370>.
54. Smith MZ, Fernandez CS, Chung A, Dale CJ, De Rose R, Lin J, Brooks AG, Krebs KC, Watkins DJ, O'Connor DH, Davenport MP, Kent SJ. 2005. The pigtail macaque MHC class I allele Mane-A*10 presents an immunodominant SIV Gag epitope: identification, tetramer development and implications of immune escape and reversion. *J Med Primatol* 34:282–293. <http://dx.doi.org/10.1111/j.1600-0684.2005.00126.x>.
55. Mankowski JL, Queen SE, Fernandez CS, Tarwater PM, Karper JM, Adams RJ, Kent SJ. 2008. Natural host genetic resistance to lentiviral CNS disease: a neuroprotective MHC class I allele in SIV-infected macaques. *PLoS One* 3:e3603. <http://dx.doi.org/10.1371/journal.pone.0003603>.
56. Borda JT, Alvarez X, Kondova I, Aye P, Simon MA, Desrosiers RC, Lackner AA. 2004. Cell tropism of simian immunodeficiency virus in culture is not predictive of in vivo tropism or pathogenesis. *Am J Pathol* 165:2111–2122. [http://dx.doi.org/10.1016/S0002-9440\(10\)63261-0](http://dx.doi.org/10.1016/S0002-9440(10)63261-0).
57. Chalifoux LV, Simon MA, Pauley DR, MacKey JJ, Wyand MS, Ringler DJ. 1992. Arteriopathy in macaques infected with simian immunodeficiency virus. *Lab Invest* 67:338–349.
58. Yanai T, Lackner AA, Sakai H, Masegi T, Simon MA. 2006. Systemic

- arteriopathy in SIV-infected rhesus macaques (*Macaca mulatta*). *J Med Primatol* 35:106–112. <http://dx.doi.org/10.1111/j.1600-0684.2005.00145.x>.
59. Li Q, Duan L, Estes JD, Ma ZM, Rourke T, Wang Y, Reilly C, Carlis J, Miller CJ, Haase AT. 2005. Peak SIV replication in resting memory CD4⁺ T cells depletes gut lamina propria CD4⁺ T cells. *Nature* 434: 1148–1152.
 60. Brechley JM, Price DA, Douek DC. 2006. HIV disease: fallout from a mucosal catastrophe? *Nat Immunol* 7:235–239. <http://dx.doi.org/10.1038/nri1316>.
 61. Mehandru S, Poles MA, Tenner-Racz K, Horowitz A, Hurley A, Hogan C, Boden D, Racz P, Markowitz M. 2004. Primary HIV-1 infection is associated with preferential depletion of CD4⁺ T lymphocytes from effector sites in the gastrointestinal tract. *J Exp Med* 200:761–770. <http://dx.doi.org/10.1084/jem.20041196>.
 62. Guadalupe M, Reay E, Sankaran S, Prindiville T, Flamm J, McNeil A, Dandekar S. 2003. Severe CD4⁺ T-cell depletion in gut lymphoid tissue during primary human immunodeficiency virus type 1 infection and substantial delay in restoration following highly active antiretroviral therapy. *J Virol* 77:11708–11717. <http://dx.doi.org/10.1128/JVI.77.21.11708-11717.2003>.
 63. Douek D. 2007. HIV disease progression: immune activation, microbes, and a leaky gut. *Top HIV Med* 15:114–117.
 64. Johnson WE, Desrosiers RC. 2002. Viral persistence: HIV's strategies of immune system evasion. *Annu Rev Med* 53:499–518. <http://dx.doi.org/10.1146/annurev.med.53.082901.104053>.
 65. Alexander L, Illyinskii PO, Lang SM, Means RE, Lifson J, Mansfield K, Desrosiers RC. 2003. Determinants of increased replicative capacity of serially passaged simian immunodeficiency virus with nef deleted in rhesus monkeys. *J Virol* 77:6823–6835. <http://dx.doi.org/10.1128/JVI.77.12.6823-6835.2003>.
 66. Ng CT, Snell LM, Brooks DG, Oldstone MB. 2013. Networking at the level of host immunity: immune cell interactions during persistent viral infections. *Cell Host Microbe* 13:652–664. <http://dx.doi.org/10.1016/j.chom.2013.05.014>.
 67. Wei X, Decker JM, Wang S, Hui H, Kappes JC, Wu X, Salazar-Gonzalez JF, Salazar MG, Kilby JM, Saag MS, Komarova NL, Nowak MA, Hahn BH, Kwong PD, Shaw GM. 2003. Antibody neutralization and escape by HIV-1. *Nature* 422:307–312. <http://dx.doi.org/10.1038/nature01470>.
 68. Overbaugh J, Morris L. 2012. The antibody response against HIV-1. *Cold Spring Harb Perspect Med* 2:a007039. <http://dx.doi.org/10.1101/cshperspect.a007039>.
 69. Burns DP, Desrosiers RC. 1991. Selection of genetic variants of simian immunodeficiency virus in persistently infected rhesus monkeys. *J Virol* 65:1843–1854.
 70. Overbaugh J, Rudensky LM, Papenhausen MD, Benveniste RE, Morton WR. 1991. Variation in simian immunodeficiency virus env is confined to V1 and V4 during progression to simian AIDS. *J Virol* 65:7025–7031.
 71. Picker LJ, Hansen SG, Lifson JD. 2012. New paradigms for HIV/AIDS vaccine development. *Annu Rev Med* 63:95–111. <http://dx.doi.org/10.1146/annurev-med-042010-085643>.
 72. O'Connor DH, Allen TM, Vogel TU, Jing P, DeSouza IP, Dodds E, Dunphy EJ, Melsaether C, Mothe B, Yamamoto H, Horton H, Wilson N, Hughes AL, Watkins DI. 2002. Acute phase cytotoxic T lymphocyte escape is a hallmark of simian immunodeficiency virus infection. *Nat Med* 8:493–499. <http://dx.doi.org/10.1038/nm0502-493>.
 73. Boutwell CL, Rolland MM, Herbeck JT, Mullins JI, Allen TM. 2010. Viral evolution and escape during acute HIV-1 infection. *J Infect Dis* 202(Suppl 2):S309–S314. <http://dx.doi.org/10.1086/655653>.
 74. Jin X, Bauer DE, Tuttleton SE, Lewin S, Gettie A, Blanchard J, Irwin CE, Safritz JT, Mittler J, Weinberger L, Kostrikis LG, Zhang L, Perelson AS, Ho DD. 1999. Dramatic rise in plasma viremia after CD8(+) T cell depletion in simian immunodeficiency virus-infected macaques. *J Exp Med* 189:991–998. <http://dx.doi.org/10.1084/jem.189.6.991>.
 75. Schmitz JE, Kuroda MJ, Santra S, Sasseville VG, Simon MA, Lifton MA, Racz P, Tenner-Racz K, Dalesandro M, Scallan BJ, Ghayeb J, Forman MA, Montefiori DC, Rieber EP, Letvin NL, Reimann KA. 1999. Control of viremia in simian immunodeficiency virus infection by CD8⁺ lymphocytes. *Science* 283:857–860. <http://dx.doi.org/10.1126/science.283.5403.857>.
 76. Ferre AL, Hunt PW, Critchfield JW, Young DH, Morris MM, Garcia JC, Pollard RB, Yee HF, Jr, Martin JN, Deeks SG, Shacklett BL. 2009. Mucosal immune responses to HIV-1 in elite controllers: a potential correlate of immune control. *Blood* 113:3978–3989. <http://dx.doi.org/10.1182/blood-2008-10-182709>.
 77. Shacklett BL. 2010. Immune responses to HIV and SIV in mucosal tissues: 'location, location, location'. *Curr Opin HIV AIDS* 5:128–134. <http://dx.doi.org/10.1097/COH.0b013e328335c178>.
 78. Rosenberg ES, Billingsley JM, Caliendo AM, Boswell SL, Sax PE, Kalams SA, Walker BD. 1997. Vigorous HIV-1-specific CD4⁺ T cell responses associated with control of viremia. *Science* 278:1447–1450. <http://dx.doi.org/10.1126/science.278.5342.1447>.
 79. Hersperger AR, Migueles SA, Betts MR, Connors M. 2011. Qualitative features of the HIV-specific CD8⁺ T-cell response associated with immunologic control. *Curr Opin HIV AIDS* 6:169–173. <http://dx.doi.org/10.1097/COH.0b013e3283454c39>.
 80. Moore C, Sidney J, English AM, Wriston A, Hunt DF, Shabanowitz J, Southwood S, Bradley K, Lafont BA, Mothe BR, Sette A. 2012. Identification of the peptide-binding motif recognized by the pigtail macaque class I MHC molecule Mane-A1*082:01 (Mane A*0301). *Immunogenetics* 64:461–468. <http://dx.doi.org/10.1007/s00251-012-0600-x>.
 81. Bosinger SE, Li Q, Gordon SN, Klatt NR, Duan L, Xu L, Francella N, Sidahmed A, Smith AJ, Cramer EM, Zeng M, Masopust D, Carlis JV, Ran L, Vanderford TH, Paiardini M, Isett RB, Baldwin DA, Else JG, Staprans SI, Silvestri G, Haase AT, Kelvin DJ. 2009. Global genomic analysis reveals rapid control of a robust innate response in SIV-infected sooty mangabeys. *J Clin Invest* 119:3556–3572. <http://dx.doi.org/10.1172/JCI40115>.
 82. Fonseca SG, Procopio FA, Goulet JP, Yassine-Diab B, Ancuta P, Sekaly RP. 2011. Unique features of memory T cells in HIV elite controllers: a systems biology perspective. *Curr Opin HIV AIDS* 6:188–196. <http://dx.doi.org/10.1097/COH.0b013e32834589a1>.
 83. Harris LD, Tabb B, Sodora DL, Paiardini M, Klatt NR, Douek DC, Silvestri G, Muller-Trutwin M, Vasile-Pandrea I, Apetrei C, Hirsch V, Lifson J, Brechley JM, Estes JD. 2010. Downregulation of robust acute type I interferon responses distinguishes nonpathogenic simian immunodeficiency virus (SIV) infection of natural hosts from pathogenic SIV infection of rhesus macaques. *J Virol* 84:7886–7891. <http://dx.doi.org/10.1128/JVI.02612-09>.
 84. Brechley JM, Silvestri G, Douek DC. 2010. Nonprogressive and progressive primate immunodeficiency lentivirus infections. *Immunity* 32: 737–742. <http://dx.doi.org/10.1016/j.immuni.2010.06.004>.
 85. Sauter MM, Pelchen-Matthews A, Bron R, Marsh M, LaBranche CC, Vance PJ, Romano J, Haggarty BS, Hart TK, Lee WM, Hoxie JA. 1996. An internalization signal in the simian immunodeficiency virus transmembrane protein cytoplasmic domain modulates expression of envelope glycoproteins on the cell surface. *J Cell Biol* 132:795–811. <http://dx.doi.org/10.1083/jcb.132.5.795>.
 86. Byland R, Vance PJ, Hoxie JA, Marsh M. 2007. A conserved dileucine motif mediates clathrin and AP-2-dependent endocytosis of the HIV-1 envelope protein. *Mol Biol Cell* 18:414–425.
 87. Bowers K, Pelchen-Matthews A, Honing S, Vance PJ, Creary L, Haggarty BS, Romano J, Ballensiefen W, Hoxie JA, Marsh M. 2000. The simian immunodeficiency virus envelope glycoprotein contains multiple signals that regulate its cell surface expression and endocytosis. *Traffic* 1:661–674. <http://dx.doi.org/10.1034/j.1600-0854.2000.010810.x>.
 88. Rowell JF, Stanhope PE, Siliciano RF. 1995. Endocytosis of endogenously synthesized HIV-1 envelope protein. Mechanism and role in processing for association with class II MHC. *J Immunol* 155:473–488.
 89. Ohno H, Aguilar RC, Fournier MC, Hennecke S, Cosson P, Bonifacio JS. 1997. Interaction of endocytic signals from the HIV-1 envelope glycoprotein complex with members of the adaptor medium chain family. *Virology* 238:305–315. <http://dx.doi.org/10.1006/viro.1997.8839>.
 90. Wyss S, Berlioz-Torrent C, Boge M, Blot G, Honing S, Benarous R, Thali M. 2001. The highly conserved C-terminal dileucine motif in the cytosolic domain of the human immunodeficiency virus type 1 envelope glycoprotein is critical for its association with the AP-1 clathrin adaptor [correction of adaptor]. *J Virol* 75:2982–2992. <http://dx.doi.org/10.1128/JVI.75.6.2982-2992.2001>.
 91. Marsh M, Pelchen-Matthews A, Hoxie JA. 1997. Roles for endocytosis in lentiviral replication. *Trends Cell Biol* 7:1–4. [http://dx.doi.org/10.1016/S0962-8924\(97\)20038-3](http://dx.doi.org/10.1016/S0962-8924(97)20038-3).
 92. Rowell JF, Ruff AL, Guarnieri FG, Staveley-O'Carroll K, Lin X, Tang J, August JT, Siliciano RF. 1995. Lysosome-associated membrane pro-

- tein-1-mediated targeting of the HIV-1 envelope protein to an endosomal/lysosomal compartment enhances its presentation to MHC class II-restricted T cells. *J Immunol* 155:1818–1828.
93. Shim H, Chauhan S, Ryoou D, Bowers K, Thomas SM, Canada KA, Burken JG, Wood TK. 2000. Rhizosphere competitiveness of trichloroethylene-degrading, poplar-colonizing recombinant bacteria. *Appl Environ Microbiol* 66:4673–4678. <http://dx.doi.org/10.1128/AEM.66.11.4673-4678.2000>.
 94. Blum JS, Wearsch PA, Cresswell P. 2013. Pathways of antigen processing. *Annu Rev Immunol* 31:443–473. <http://dx.doi.org/10.1146/annurev-immunol-032712-095910>.
 95. Rucker J, Doranz BJ, Edinger AL, Long D, Berson JF, Doms RW. 1997. Cell-cell fusion assay to study role of chemokine receptors in human immunodeficiency virus type 1 entry. *Methods Enzymol* 288:118–133.
 96. Lodge R, Lalonde JP, Lemay G, Cohen EA. 1997. The membrane-proximal intracytoplasmic tyrosine residue of HIV-1 envelope glycoprotein is critical for basolateral targeting of viral budding in MDCK cells. *EMBO J* 16:695–705. <http://dx.doi.org/10.1093/emboj/16.4.695>.
 97. Lodge R, Delamarre L, Lalonde JP, Alvarado J, Sanders DA, Dokheler MC, Cohen EA, Lemay G. 1997. Two distinct oncornaviruses harbor an intracytoplasmic tyrosine-based basolateral targeting signal in their viral envelope glycoprotein. *J Virol* 71:5696–5702.
 98. Ball JM, Mulligan MJ, Compans RW. 1997. Basolateral sorting of the HIV type 2 and SIV envelope glycoproteins in polarized epithelial cells: role of the cytoplasmic domain. *AIDS Res Hum Retroviruses* 13:665–675. <http://dx.doi.org/10.1089/aid.1997.13.665>.
 99. Postler TS, Desrosiers RC. 2013. The tale of the long tail: the cytoplasmic domain of HIV-1 gp41. *J Virol* 87:2–15. <http://dx.doi.org/10.1128/JVI.02053-12>.
 100. Sandler NG, Bosinger SE, Estes JD, Zhu RT, Tharp GK, Boritz E, Levin D, Wijeyesinghe S, Makamdop KN, del Prete GQ, Hill BJ, Timmer JK, Reiss E, Yarden G, Darko S, Contijoch E, Todd JP, Silvestri G, Nason M, Norgren RB, Jr, Keele BF, Rao S, Langer JA, Lifson JD, Schreiber G, Douek DC. 2014. Type I interferon responses in rhesus macaques prevent SIV infection and slow disease progression. *Nature* 511:601–605. <http://dx.doi.org/10.1038/nature13554>.
 101. Soulas C, Conerly C, Kim WK, Burdo TH, Alvarez X, Lackner AA, Williams KC. 2011. Recently infiltrating MAC387(+) monocytes/macrophages a third macrophage population involved in SIV and HIV encephalitic lesion formation. *Am J Pathol* 178:2121–2135. <http://dx.doi.org/10.1016/j.ajpath.2011.01.023>.
 102. Burdo TH, Lackner A, Williams KC. 2013. Monocyte/macrophages and their role in HIV neuropathogenesis. *Immunol Rev* 254:102–113. <http://dx.doi.org/10.1111/imr.12068>.
 103. Calantone N, Wu F, Klase Z, Deleage C, Perkins M, Matsuda K, Thompson EA, Ortiz AM, Vinton CL, Ourmanov I, Lore K, Douek DC, Estes JD, Hirsch VM, Brechley JM. 2014. Tissue myeloid cells in SIV-infected primates acquire viral DNA through phagocytosis of infected T cells. *Immunity* 41:493–502. <http://dx.doi.org/10.1016/j.immuni.2014.08.014>.
 104. Westmoreland SV, Converse AP, Hrecka K, Hurley M, Knight H, Piatak M, Lifson J, Mansfield KG, Skowronski J, Desrosiers RC. 2014. SIV vpx is essential for macrophage infection but not for development of AIDS. *PLoS One* 9:e84463. <http://dx.doi.org/10.1371/journal.pone.0084463>.
 105. Mica L, Vomela J, Keel M, Trentz O. 2014. The impact of body mass index on the development of systemic inflammatory response syndrome and sepsis in patients with polytrauma. *Injury* 45:253–258. <http://dx.doi.org/10.1016/j.injury.2012.11.015>.
 106. Gramberg T, Kahle T, Bloch N, Wittmann S, Mullers E, Daddacha W, Hofmann H, Kim B, Lindemann D, Landau NR. 2013. Restriction of diverse retroviruses by SAMHD1. *Retrovirology* 10:26. <http://dx.doi.org/10.1186/1742-4690-10-26>.
 107. Diamond MS, Farzan M. 2013. The broad-spectrum antiviral functions of IFIT and IFITM proteins. *Nat Rev Immunol* 13:46–57. <http://dx.doi.org/10.1038/nri3344>.
 108. Alcántara S, Reece J, Amarasena T, Rose RD, Manitta J, Amin J, Kent SJ. 2009. Thrombocytopenia is strongly associated with simian AIDS in pigtail macaques. *J Acquir Immune Defic Syndr* 51:374–379. <http://dx.doi.org/10.1097/QAI.0b013e3181a9cbcf>.
 109. Davey RT, Jr, Bhat N, Yoder C, Chun TW, Metcalf JA, Dewar R, Natarajan V, Lempicki RA, Adelsberger JW, Miller KD, Kovacs JA, Polis MA, Walker RE, Falloon J, Masur H, Gee D, Baseler M, Dimitrov DS, Fauci AS, Lane HC. 1999. HIV-1 and T cell dynamics after interruption of highly active antiretroviral therapy (HAART) in patients with a history of sustained viral suppression. *Proc Natl Acad Sci U S A* 96:15109–15114. <http://dx.doi.org/10.1073/pnas.96.26.15109>.
 110. Chun TW, Justement JS, Murray D, Hallahan CW, Maenza J, Collier AC, Sheth PM, Kaul R, Ostrowski M, Moir S, Kovacs C, Fauci AS. 2010. Rebound of plasma viremia following cessation of antiretroviral therapy despite profoundly low levels of HIV reservoir: implications for eradication. *AIDS* 24:2803–2808. <http://dx.doi.org/10.1097/QAD.0b013e328340a239>.
 111. Hong FF, Mellors JW. 2015. Changes in HIV reservoirs during long-term antiretroviral therapy. *Curr Opin HIV AIDS* 10:43–48. <http://dx.doi.org/10.1097/COH.000000000000119>.
 112. Palmer S, Josefsson L, Coffin JM. 2011. HIV reservoirs and the possibility of a cure for HIV infection. *J Intern Med* 270:550–560. <http://dx.doi.org/10.1111/j.1365-2796.2011.02457.x>.
 113. Del Prete GQ, Shoemaker R, Oswald K, Lara A, Trubey CM, Fast R, Schneider DK, Kiser R, Coalter V, Wiles A, Wiles R, Freemire B, Keele BF, Estes JD, Quinones OA, Smedley J, Macallister R, Sanchez RI, Wai JS, Tan CM, Alvord WG, Hazuda DJ, Piatak M, Jr, Lifson JD. 2014. Effect of suberoylanilide hydroxamic acid (SAHA) administration on the residual virus pool in a model of combination antiretroviral therapy-mediated suppression in SIVmac239-infected Indian rhesus macaques. *Antimicrob Agents Chemother* 58:6790–6806. <http://dx.doi.org/10.1128/AAC.03746-14>.
 114. Archin NM, Sung JM, Garrido C, Soriano-Sarabia N, Margolis DM. 2014. Eradicating HIV-1 infection: seeking to clear a persistent pathogen. *Nat Rev Microbiol* 12:750–764. <http://dx.doi.org/10.1038/nrmicro3352>.
 115. Hansen SG, Ford JC, Lewis MS, Ventura AB, Hughes CM, Coyne-Johnson L, Whizin N, Oswald K, Shoemaker R, Swanson T, Legasse AW, Chiuchiolo MJ, Parks CL, Axthelm MK, Nelson JA, Jarvis MA, Piatak M, Jr, Lifson JD, Picker LJ. 2011. Profound early control of highly pathogenic SIV by an effector memory T-cell vaccine. *Nature* 473:523–527. <http://dx.doi.org/10.1038/nature10003>.
 116. Fukazawa Y, Park H, Cameron MJ, Lefebvre F, Lum R, Coombes N, Mahyari E, Hagen SI, Bae JY, Reyes MD 3rd, Swanson T, Legasse AW, Sylwester A, Hansen SG, Smith AT, Stafova P, Shoemaker R, Li Y, Oswald K, Axthelm MK, McDermott A, Ferrari G, Montefiori DC, Edlefsen PT, Piatak M, Jr, Lifson JD, Sekaly RP, Picker LJ. 2012. Lymph node T cell responses predict the efficacy of live attenuated SIV vaccines. *Nat Med* 18:1673–1681. <http://dx.doi.org/10.1038/nm.2934>.
 117. Johnson RP, Desrosiers RC. 1998. Protective immunity induced by live attenuated simian immunodeficiency virus. *Curr Opin Immunol* 10:436–443. [http://dx.doi.org/10.1016/S0952-7915\(98\)80118-0](http://dx.doi.org/10.1016/S0952-7915(98)80118-0).
 118. George MD, Hu W, Billingsley JM, Reeves RK, Sankaran-Walters S, Johnson RP, Dandekar S. 2014. Transcriptional profiling of peripheral CD8+ T cell responses to SIVDelta_{nef} and SIVmac251 challenge reveals a link between protective immunity and induction of systemic immunoregulatory mechanisms. *Virology* 468-470C:581–591.
 119. Reynolds MR, Weiler AM, Piaskowski SM, Kolar HL, Hessel AJ, Weiker M, Weisgrau KL, Leon EJ, Rogers WE, Makowsky R, McDermott AB, Boyle R, Wilson NA, Allison DB, Burton DR, Koff WC, Watkins DI. 2010. Macaques vaccinated with simian immunodeficiency virus SIVmac239Delta_{nef} delay acquisition and control replication after repeated low-dose heterologous SIV challenge. *J Virol* 84:9190–9199. <http://dx.doi.org/10.1128/JVI.00041-10>.
 120. Reynolds MR, Weiler AM, Weisgrau KL, Piaskowski SM, Furlott JR, Weinfurter JT, Kaizu M, Soma T, Leon EJ, MacNair C, Leaman DP, Zwick MB, Gostick E, Musani SK, Price DA, Friedrich TC, Rakasz EG, Wilson NA, McDermott AB, Boyle R, Allison DB, Burton DR, Koff WC, Watkins DI. 2008. Macaques vaccinated with live-attenuated SIV control replication of heterologous virus. *J Exp Med* 205:2537–2550. <http://dx.doi.org/10.1084/jem.20081524>.
 121. Wyand MS, Manson K, Montefiori DC, Lifson JD, Johnson RP, Desrosiers RC. 1999. Protection by live, attenuated simian immunodeficiency virus against heterologous challenge. *J Virol* 73:8356–8363.